Chapter 7

Graphene Quantum Dots - From Emergence to Nanotheranostic Applications

Preeti Nigam Joshi, Subir Kundu, Sunil K. Sanghi and Dhiman Sarkar

Additional information is available at the end of the chapter

http://dx.doi.org/10.5772/61932

Abstract

Quantum dots are at the cutting edge of nanotechnology development. Due to their unique optical and physical properties, they have potential applications in many avenues of medicine and biotechnology. With the advancements in nano-sciences, novel applications of quantum dots are constantly being explored for drug delivery and bioimaging. Graphene quantum dots (GQDs) are nanoparticles of graphene with properties of quantum dots as well as graphene. GQDs have ignited remarkable research interest in the field of medicine and biology and are considered as well-suited candidates for nanotheranostic applications due to their excellent biocompatibility and tunable physicochemical properties. The promising emerging implications of GQD platforms for diagnostics and therapeutics advances are the basis of this chapter.

Keywords: Graphene quantum dots, Nanotheranostics, Bioimaging, Smart Materials

1. Introduction

Nanotechnology is undoubtedly the most promising research arena that has deeply influenced biotechnology and medicinal fields and can be considered as the prime technology of the 21st century. Not only biological endeavors, nanotechnology facilitates innovative techniques and applications in electronics, computer science, and aerospace technology also. In the present socioeconomical scenario, nanotechnology can play a significant role in solving many health and environmental issues. "Nano" is a Latin word meaning "dwarf" and technically, an object having one dimension in nano size is considered a nanomaterial. At nanoscale, the physicochemical properties of a substance change drastically like surface area enhancement; changes in thermal and optical properties and dominance of quantum effect are associated with the conversion of a substance to nanoscale. The concept of nanotechnology was first described by

physicist Richard P. Fenyman in 1959 and the term nanotechnology itself was coined by Norio Taniguchi in 1974.

From its evolution, to date, nanotechnology has marked its significant presence in diverse areas of medicines, biology, electronics, space research, and agriculture.

In the field of medical science and health care sector, nanotechnology intervention has created a new field called "nanomedicine." The most prominent areas of nanotechnology application in pharmaceutical industry include drug delivery, biosensors, and diagnostic imaging. Different nanoparticles (metal, polymeric, liposomes, and dendrimers) already have well-established applications in drug delivery and disease diagnostics, but in this chapter we will mainly focus on the applications of graphene quantum dots (GQDs) in drug delivery and bioimaging.

1.1. History and evolution of graphene quantum dots

In general, a quantum dot (QD) is a semiconductor crystal in the size range of 1–10 nm. Due to their specific size range, QD exhibits quantum phenomena that yield significant benefits in optical properties. It is a well-known fact that on excitation, smaller the size of QD higher will be the energy and intensity of emitted light. QDs can be derived from metals (gold), semiconductors (e.g., selenium, cadmium, etc.), or carbon-based materials (carbon dots and graphene). Due to their specific properties, QDs are used as photodiodes and have a wide range of applications in analytical chemistry but the potential toxicity associated with semiconductor quantum dots prevents their applicability in biology and medicine. This limitation of QDs was the prime driving source for finding out new alternatives, and with the advancement in nanotechnology, quantum dots fabricated from graphene evolved as a more biocompatible source for biomedical applications. Graphene is a carbon-allotrope, zero-band-gap, two-dimensional (2D) sheet of a single layer sp^2-hybridized carbon with excellent thermoelectric properties [1, 2]. First, its properties were studied by R. Wallace in 1947 [3], and Hoffman et al. isolated pure graphene from graphene oxide via hydrazine reduction in 1963 [4]. The name "graphene" was given by Mouras et al. in 1987 [5]. Though initial discoveries on graphene were mostly unnoticed, it is only after the groundbreaking work by Geim and Novoselov in isolating graphene from highly oriented pyrolytic graphite (HOPG) that huge interest in research was ignited exploring the properties of graphene [2].

GQDs, first reported by Peng et al., are zero-dimensional graphene segments that are small enough to exhibit quantum confinement and size effect. Unlike graphene sheets, they exhibit band gap that is responsible for their unique electrical and optoelectronic properties. Moreover, GQDs also possess size-dependent strong photoluminescence properties [6–9]. These are relatively new nano-dimension entities with a size range between 1 and 10 nm, having a "molecule-like structure," nontoxic, and can be easily handled compared with colloidal QDs. GQDs are gradually attaining significance due to their potential applications in sensors, electronics, and biology from the standpoint of less health concerns than their traditional semiconductor counterparts due to their less toxicity, ease of functionalization, and favorable electro-optic properties [10–12].

http://dx.doi.org/10.5772/61932

2. Synthesis methodologies for graphene quantum dots

To date, remarkable progress has been made in developing new synthesis methodology for graphene quantum dots. There are two broad synthesis approaches for GQDs that can be classified as top-down and bottom-up methods. The first route is based on the cleavage and exfoliation of bulk graphene-based material (graphite) under harsh conditions. In the bottom-up approach, GQDs are mostly prepared from polycyclic aromatic compounds or molecules with aromatic structures.

Though the top-down method is more cost effective having multiple synthesis steps, harsh reaction conditions and lack of morphological control are the major shortcomings associated with this method. However, the prime advantage with this approach is that GQDs obtained by this method have oxygen-containing functional groups influencing the solubility and functionalization of GQDs. Bottom-up approaches give precise control on morphology, size, and shape but still suffer from disadvantages like need for expensive precursors and complex synthesis steps. GQDs synthesized by this method have a strong tendency of aggregation that limits the applicability of this approach. In this segment, a brief overview of recent approaches for GQD synthesis will be given.

2.1. Top-down approaches

The basic route of implementing top-down methods is either chemical reactions or physical methods. Based on their mechanism, these approaches can be described as "defect-mediated fragmentation processes." Mostly, chemical approaches are applied due to some distinguished benefits. Generally, graphene oxide (GO) is cleaved to generate GQDs, and chemical methods generate defects due to the presence of oxygen-containing reactive epoxy and hydroxyl groups. The reactive groups generate a cleavage site, thus allowing GO sheets to be cut into smaller sheets [13]. During the oxidation procedure of graphene, epoxy groups appear linearly on the carbon lattice and this alignment causes the cleavage of C–C bond. The emergence of epoxy groups on GO makes it energetically favorable to convert these groups into stable carbonyl pairs at room temperature. Graphene sheets become fragile due to these chemical transformation and defects and can be readily attacked by chemicals to generate GQDs. The presence of aromatic sp^2 domains having epoxy groups on graphene, GO, carbon black, and carbon nanotubes makes them excellent starting candidates for GQD synthesis.

2.1.1. Hydrothermal and solvothermal synthesis

Particle size of GQDs and formation mechanisms are deeply influenced by hydrothermal synthesis. Water, as a green solvent used in this procedure, is a key player in atom-economical reactions [14]. These methods generally require a high amount of strong alkali (NaOH and ammonia) for cutting carbon precursors into GQDs. First, Pan et al. reported this method to synthesize water-soluble blue luminescent quantum dots. The diameter of QDs was 5–13 nm and they exhibited strong fluorescence in alkali conditions, while in acidic conditions the fluorescence got quenched. The basic synthesis step involved was the oxidation of graphite to GO that produces epoxy groups, which cause the rupture of C–C bonds. Further, these epoxy

groups are oxidized into stable carbonyl groups responsible for the water dispersiblity of GQDs as shown in Figure 1. Later, Pan et al. put forth a modified high-temperature synthesis procedure to synthesize fine crystalline GQDs with green fluorescence [14, 15].

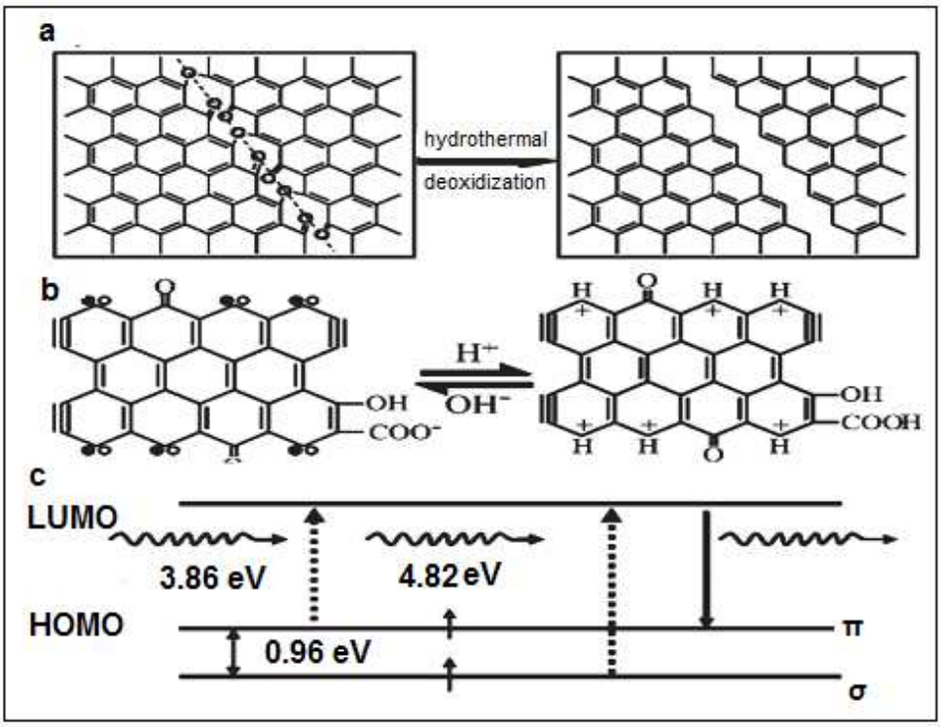

Figure 1. Synthesis mechanism of GQDs via cutting of graphite sheets. This was a multistep process and GQDs were prepared by the reduction of epoxy groups generated in oxidation and cutting step. (Ref [14]: Pan et al.)

In recent years, graphene-based materials have seen extensive applications in the field of electronics, pollution treatment, solar cells, Li-ion batteries, and sensing. The modification of graphene by nitrogen or boron doping significantly amends its optical and electronic properties. Similarly, a change in photoluminescence and electric properties can be attained by tuning the band gap of GQDs [16].

Hydrothermal approach deeply influences the size and morphology of GQDs. In one report, Tetsuka et al. [17] synthesized amine-functionalized graphene quantum dots (NH_2-GQDs) using oxidized graphene sheets and ammonia using this method by bond–scission reaction. Concentration variation of ammonia played a key role in controlling the luminescence of GQDs from violet to yellow. The nucleophilic substitution upon ammonia addition to graphene triggered the reaction of ring-opening epoxide, and sp^2 domains were cut out to generate amino-functionalized GQDs of 2.5 nm size and 1.1 nm thickness (Figure 2). In this series, few researchers have reported altered optical properties of GQDs after functionalization with polymers or small molecules. Feng et al. have put forth their idea of fluorinated GQDs (F-GQDs) prepared by hydrothermal procedure. Xenon difluoride was utilized for fluorinated graphene synthesis at high temperatures and then F-GQDs were obtained by hydrothermal procedure [18].

http://dx.doi.org/10.5772/61932

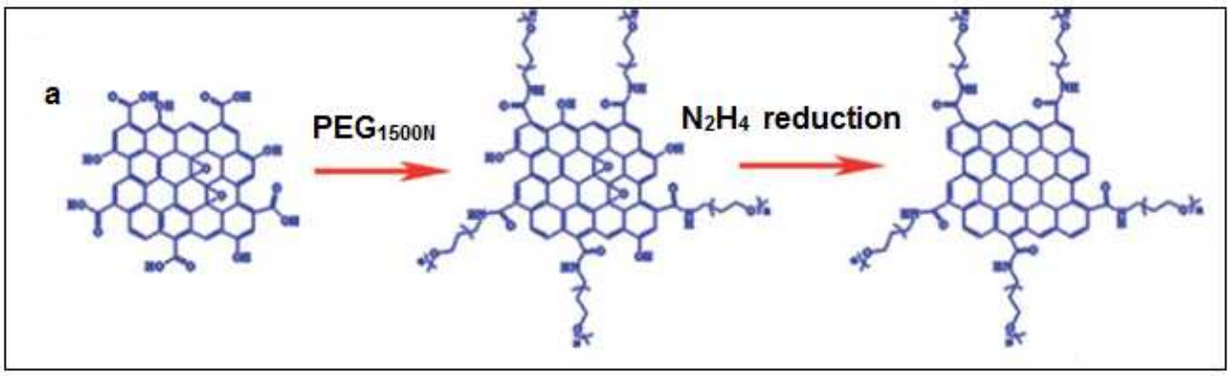

Figure 3. Synthesis of surface-passivated GQDs with hydrazine hydrate reduction and surface passivation by PEG_{1500N}. (Ref. [23]: Shen et al.)

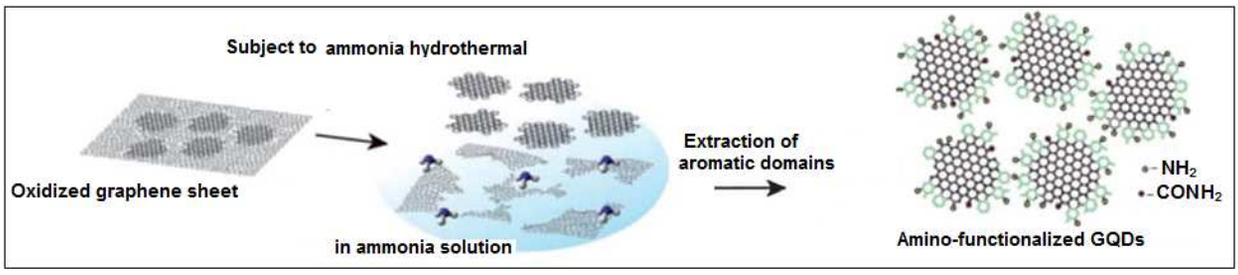

Figure 2. Illustration of hydrothermal synthesis of amino-functionalized GQDs. (Ref [17]: Tetsuka et al.)

Hu et al. [19] came up with a new methodology by synthesizing nitrogen-doped GQDs (N-GQDs) from oxidized debris (ODs) on graphene oxide by the hydrothermal treatment of GO at 180°C in the presence of ammonia without any strong acid treatment. The as-prepared N-GQDs were highly blue luminescent, 2–6 nm in size, with a quantum yield (QY) of 24.6. Aqueous route and novel application of ODs for the synthesis of N-GQDs were the major highlights of their work. The prime advantage associated with this approach was its cost effectiveness due to aqueous reaction conditions in the absence of any surface-passivation agent or strong acids. Liu et al. and Zhang and coworkers also reported similar procedures for the synthesis of functionalized GQDs [20, 21]. Recently, Nigam et al. have reported a novel reducing agent Lawsone for hydrothermal synthesis of GQDs of 3-6 nm size and green fluorescence from graphene oxide reduction. The GQDs were stable and showed good biocompatibility at higher concentrations [22]. In another approach, Shen et al. prepared surface-passivated GQDs from hydrazine hydrate reduction of GO that were further passivated by poly(ethylene glycol) diamine (PEG_{1500N}) as depicted in Figure 3. By this method, they obtained GQDs of broad diameter in the range of 5–19 nm with blue fluorescence; hence, they further modified the procedure, and the GQDs were synthesized via one-pot hydrothermal synthesis route using GO and PEG as starting materials. The basic advantage of PEG-surface passivation was high photoluminescence (PL) quantum yield, better photon-to-electron conversion, and improved unconverted PL properties than native GQDs [23].

In solvothermal reaction, organic solvents (dimethyl sulfoxide (DMSO), dimethylformamide (DMF), and benzene) are utilized instead of water to obtain GQDs. The size and morphology of the GQDs are greatly influenced by the physicochemical properties of solvents. In a recent approach reported by Zhu et al. [24], DMF was used as a solvent to split graphene oxide into green fluorescent GQDs under ultrasonication followed by heating at 200°C in a Teflon autoclave. Column chromatography on silica gel was performed to obtain GQDs instead of dialysis treatment with water as eluent. As an improvisation, they later increased the reaction time to 8 h using methanol/methylene chloride and water as mobile phase for GQD synthesis [25]. Shin et al. put forth a new solvothermal approach based on novel acid-free and oxone-oxidant-assisted synthesis of GQDs using various natural carbon resources, including graphite, multiwall carbon nanotubes (MWCNTs), carbon fibers (CFs), and charcoal (C) [26].

2.1.2. Microwave-assisted cutting and ultrasonic approach

Hydrothermal/solvothermal techniques are the most applied processes for GQD synthesis, but due to their tedious synthesis protocols, researchers have reported a few procedures based on microwave-assisted synthesis as this technique has the advantage of both hydrothermal and microwave processes. In a recent work by Luk et al., nitrogen-doped GQDs (N-GQDs) were prepared by mixing 3 wt% of glucose dissolved in aqueous ammonia (25%) at room temperature. The homogeneous solution was heated in a microwave reactor (300 W power) for 5 min at 180°C. Using this method, GQDs with 6 nm size and excitation-dependent luminescence spectra were obtained. Upconversion emission spectrum was another important feature of their work. According to their findings, nitrogen doping played the key role in two-photon luminescence [27]. Recently, a one-step-microwave-assisted solvothermal method for fabricating sulfur- and nitrogen-doped GQDs (S-, N-GQDs) has been reported based on the reaction of GO and reduced glutathione in N,N-dimethylformamide (DMF) at 200° C under microwave irradiation [28].

Tang et al. have reported glucose-derived GQDs through a microwave-assisted hydrothermal (MAH) approach. The basic advantage of this method was uniform heating that produced particles of small sizes. The authors have synthesized GQDs of average size of 4 nm. Based on the microwave heating time, GQDs of varying sizes were obtained [29].

In another approach, Li et al. [30] have developed a method for facile microwave-assisted synthesis of two-color GQDs in acidic conditions. Figure 4 shows the schematic of basic steps involved in the synthesis procedure. Greenish yellow luminescent GQDs (gGQDs) of average size 4–5 nm were obtained. The as-synthesized GQDs were further moderately reduced with $NaBH_4$, and blue GQDs were produced with the same dimensions. The quantum yield of blue and green GQDs was 23% and 12%, respectively.

Ultrasonication is a simpler procedure to prepare GQDs, because of the fact that ultrasound can generate alternating low-pressure and high-pressure waves in liquid that can be useful for shearing the carbon layer materials into GQDs. Zhu et al. [31] have reported one-step synthesis using ultrasonication with only graphene oxide and $KMnO_4$, and luminescent graphene quantum dots of 3 nm in high quantum yield were prepared.

http://dx.doi.org/10.5772/61932

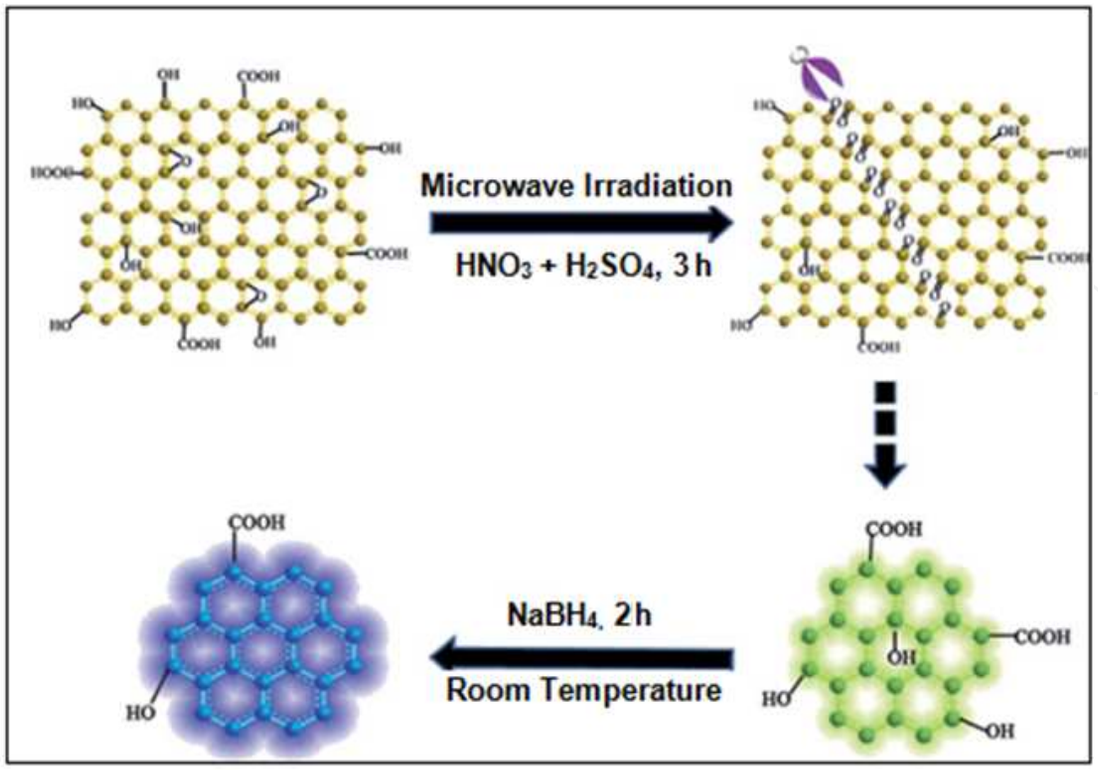

Figure 4. Schematic of synthesis of green and blue GQDs. (Ref [30]: Li et al.)

2.1.3. Electrochemical exfoliation approaches

Electrochemical approaches were already established for the synthesis of carbon dots at a potential of 1.5–3 V, where electrochemical exfoliation and intercalation are the basic steps to obtain the desired product by generating hydroxyl and oxygen radicals that play the role of electrochemical "scissors" in an oxidative cleavage reaction [32, 33].

Li et al. [34] extended this strategy further to synthesize GQDs of 3–5 nm size through an electrochemical method that involved the breaking up of a graphene film that has been treated with oxygen plasma to increase hydrophilicity. The as-synthesized GQDs exhibited green luminescence and enhanced stability in water dispersion. Zhang et al. [35] put forth another approach for synthesizing water-soluble GQDs by electrochemical exfoliation of graphite and further reducing the as-synthesized nanoscale GQDs with hydrazine at room temperature in contrast to earlier reported high-temperature reductions. It was the first report of strong yellow fluorescence in high yield and uniform sizes. The yellow fluorescence can be attributed to hydrazide groups on the surface of GQDs, produced during the low-temperature hydrazine reduction step. Though carbon nanotubes are not very suitable materials for GQD synthesis due to their potential toxicity, recently Pillai and Shinde have described an electrochemical procedure for GQDs based on multiwalled nanotubes. Figure 5 illustrates the mechanism of GQD synthesis. This method is a new procedure to synthesize size-tunable quantum dots by the oxidation time [36]. Due to the toxic base material, applicability of GQDS prepared by such methods is limited and it involves extra efforts to coat the GQDs with any polymer or com-

pound to enhance their biocompatibility. However, in another report, Shinde et al. put forth a two-step electrochemical strategy of synthesizing nitrogen-doped GQDs (N-GQDs) from multiwall CNTs. The presence of nitrogen dopants in the carbon framework caused faster unzipping of N-MWCNTs, and also provided lower activation energy site that was beneficial for enhanced electrocatalytic activity for oxygen reduction reaction [37].

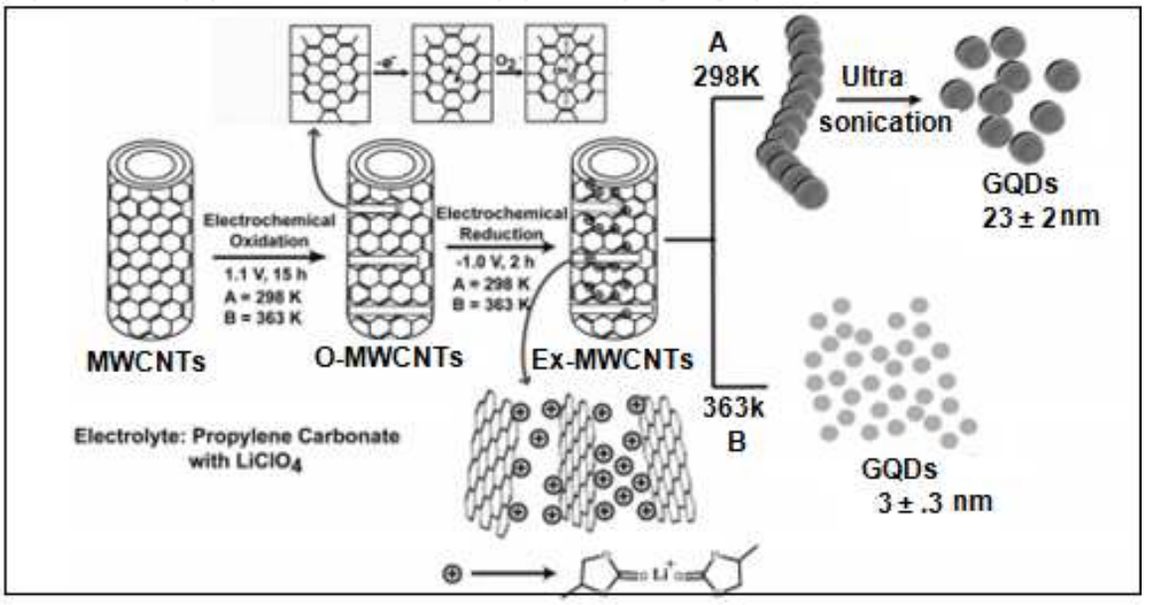

Figure 5. Synthesis stages involved in electrochemical synthesis of GQDs from MWCNTs. (Ref [36]: Shinde et al.)

Recently, a facile electrochemical exfoliation of graphite in $K_2S_2O_8$ solution for the synthesis of uniform small-sized red fluorescent GQDs (RF-GQDs) was demonstrated by Tan et al. with no chemical modification. This method was relatively simple, and water-soluble GQDs of uniform size (3 nm diameter) with excellent PL properties and less cytotoxicity were obtained with in vivo applicability in bioimaging applications.

2.1.4. Nanolithography

Nanolithography is a high-precision technique but gives low yield, and expensive instrumentation is required, which is the prime reason for very few reports being available on this methodology. Ponomarenko et al. [39] used ultrahigh-resolution electron beam lithography to cut graphene to desired sizes. In another work by Lee and coworkers [40], chemical vapor deposition method was used to generate GQDs of uniform size from self-assembled block copolymers (BCP) as an etch mask on graphene films. Although this was a low-yielding method, uniform particles were synthesized for probing effects of size and functionalization.

2.2. Bottom-up approaches

As compared to top-down approaches, very few bottom-up procedures have been reported.

http://dx.doi.org/10.5772/61932

2.2.1. Pyrolysis

Pyrolysis is one of the simplest methods of synthesizing graphene quantum dots. In this method, GQDs are formed via carbonization of small organic molecules. However, apart from its simplicity, GQDS of low quantum yield are produced in most of the cases. Few recent reports based on this method are described here. GQDs from hexa-peri-hexabenzocoronene (HBC) were reported by Liu et al. [41]. HBC is a polycyclic aromatic hydrocarbon that resembles nanoscaled fragments of graphene that stack via π–π interactions. This method produced monodisperse disk-like GQDs of ≈60 nm and 2–3 nm thickness. Pyrolysis, unfunctionalization, and oxidation processes are shown in Figure 6. Further, GQDs from citric acid (CA) and glutathione (GSH) as starting materials were also prepared. Glutathione is a tripeptide containing glutamate, cysteine, and glycine. The core advantage of glutathione is enhanced biocompatibility and high quantum yield. In this method, a 33.6% QY was obtained that can be attributed to the amination reaction between the amine group of GSH and the epoxy and carboxylic groups of GQDs [42]. It has been reported earlier that carboxylic and epoxy groups act like non-radiative electron–hole combination centers [18], and during amination reaction, reduction in number of these centers leads to better emission properties.

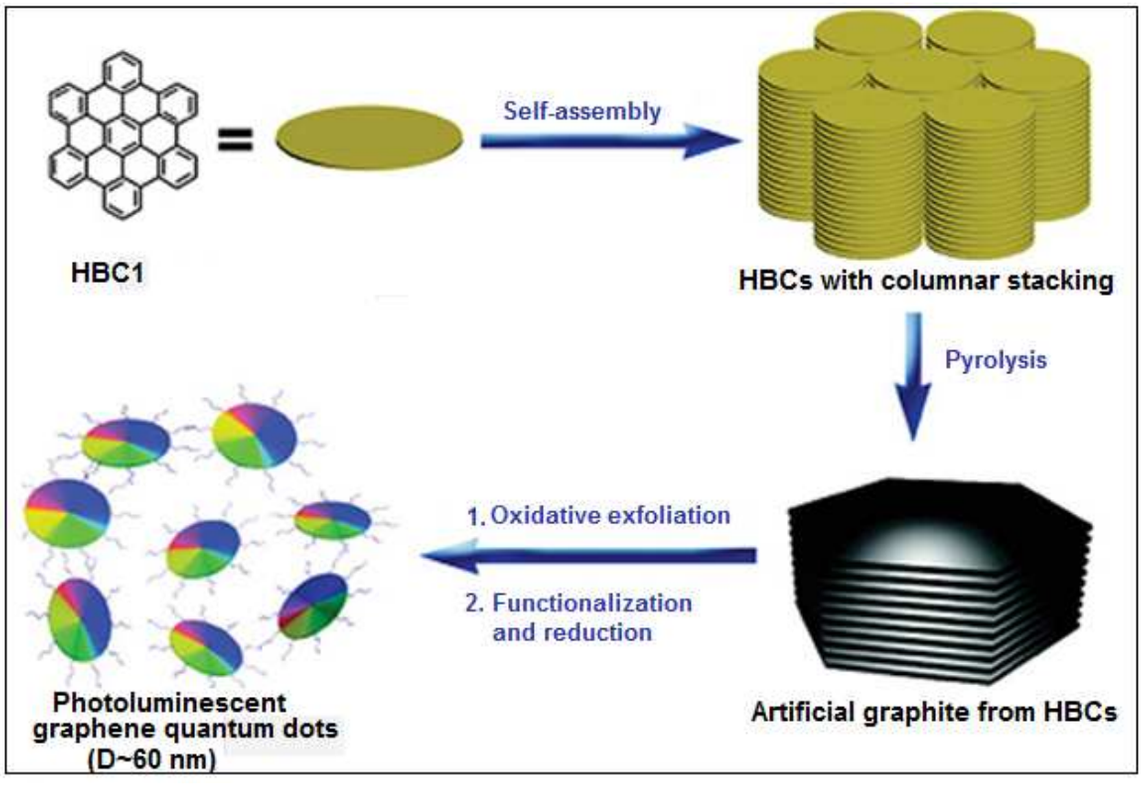

Figure 6. Illustration of pyrolysis procedure of HBC for synthesis of GQDs. Monodisperse disk like GQDs with 2–3 nm thickness and 60 nm diameters were obtained. (Ref [41]: Liu et al.)

In another approach, Wu and coworkers synthesized GQDs via a simple one-step pyrolysis of L-glutamic acid in a heating mantle. With this method, GQDs with a broad emission range

(from visible to near infrared (NIR)) with excellent quantum yield of 55% were obtained. Figure 7a illustrates the basic steps of pyrolysis procedure, while Figure 7 b, c depicts the characteristic features of GQDs. These quantum dots exhibited tremendous bioimaging potential, and as shown in Figure 7d they can be successfully utilized for in vitro and in vivo cell imaging [43].

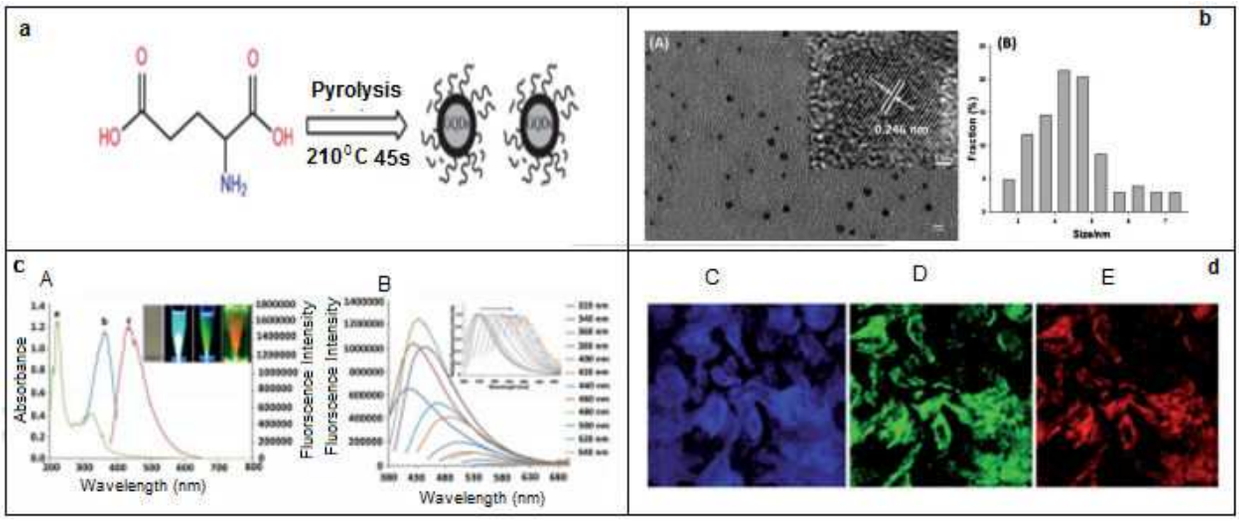

Figure 7. (a) Schematic of pyrolysis of L-glutamic acid; (b) HRTEM image of GQDs and size distribution; (c) Absorption spectra (A) and fluorescence emission spectra (B); (d) Confocal fluorescence images (C–E) under different excitation wavelengths from 359 nm, 488 nm, and 514 nm. (Ref [43]: Wu et al.)

Citric acid was also explored as the staring material to synthesize blue luminescent GQDs by tuning its carbonization degree. The as-synthesized GQDs were 15 nm in width and 0.5–2.0 nm in thickness. GQDs obtained by this method were self-passivated due to incomplete carbonization of citric acid [13]. Gram-scale synthesis of functionalized GQDs from pyrene via facile molecular fusion route was described by Wang et al. [44]. The single-crystalline GQDs were having excellent optical properties such as bright excitonic fluorescence, strong excitonic absorption bands extending to the visible region, large molar extinction coefficients, and long-term photostability.

Recently, a facile bottom-up method producing fluorescent nitrogen-doped graphene quantum dots (N-GQDs) based on one-step pyrolysis of citric acid and tris(hydroxymethyl)aminomethane was reported. These nitrogen-doped GQDs emitted strong blue fluorescence under 365 nm ultraviolet (UV) light excitation with the highest reported quantum yield of 59.2% [45].

2.2.2. From fullerene

Lu et al. [46] reported a mechanistic approach for the synthesis of geometrically well-defined GQDs on a ruthenium surface using C_{60} molecules as a precursor. Ruthenium (Ru) catalyzed the cage opening reaction of C_{60}. The strong C60–Ru interaction initiated the formation of surface vacancies in the Ru single crystal and a subsequent embedding of C60 molecules in the surface. At high temperatures, embedded molecules get fragmented and form carbon clusters that undergo diffusion and aggregation to form GQDs.

http://dx.doi.org/10.5772/61932

3. Physicochemical properties of graphene quantum dots

GQDs are nanosized graphene sheets. In this chapter, we will deal with Bohr radius and quantum confinement effect to explain the optical properties of GQDs. It is believed that the variations in photoluminescence, electronic, and physical characteristics of GQDs are related with these two important terminologies. Therefore, let us briefly look at these terms that will enhance our basic understanding on the properties of GQDs.

Bohr radius

Quantum dots possess the structural features of parent molecule but exhibit unique electrical and optical properties as a function of their size. The quantum size effect occurs when these nanostructures attain a size smaller than a fundamental unit of exciton Bohr radius. An exciton is a bound state of an electron and an electron hole, which are attracted to each other by the electrostatic Coulomb force that is formed when a photon is absorbed by a semiconductor that excites an electron from the valence band into the conduction band.

In Gaussian unit, a Bohr radius is given by:

$$a_0 = \hbar^2 / m_e e^2 \tag{1}$$

where a_0 is the Bohr radius, $\hbar$ is the reduced Plank's constant, and m_e is the electron rest mass. Bohr radius has an approximate value of 0.53 Å [47].

Quantum confinement effect

When the size of quantum dot becomes smaller and approaches toward the Bohr radius of bulk exciton, the quantum confinement effect becomes apparent. Depending on the dimension of the confinement, three kinds of structures can be defined: quantum well (QW), quantum wire (QWR), and quantum dot (QD) based on the reduced dimension. Material size is reduced in one direction in a QW and the exciton is free to move in other two directions, while in a QWR the material size is reduced in both the directions leaving only a single direction for the movement of exciton. In a QD, all directions are reduced restricting the free movement of exciton in any direction [48].

Due to this confinement effect exciton nature gets modified, which leads to distinguished optical and electrical properties of quantum dots.

3.1. Electrochemical properties

The 2010 Nobel Prize was awarded to Geim and Novoselov for their remarkable work in graphene. This not only validated the importance of graphene but also paved the way for their applications in different research areas of electronics and optics as well as commercial applications. GQDs are so closely related to graphene that a discussion on GQD would be incomplete without describing the basics of graphene. With technological advancements in different fields, demand for carbon and carbon-related materials like graphene, carbon

nanotubes is increasing rapidly for electrical, mechanical, and biomedical applications due to their tremendous thermal, electrical, mechanical, optical, and other unique properties [49–51]. Although graphene has an upper hand in comparison to CNTs due to low toxicity, it has the disadvantages of aggregation and low dispersity. The nanoparticles of GQDs are more advantageous due to their better physicochemical properties.

Graphene is known as a zero-band-gap material having infinite exciton Bohr radius, because of the linear energy dispersion of the charge carriers [52, 53]. Quantum confinement is a phenomenon that evolves in a finite-size graphene sheet and GQDs are best examples of this prominent effect. GQDs exhibit non-zero, tunable band gap than graphene and luminescence on excitation. Moreover, GQDs provide the flexibility of tuning the band gap by size and surface chemistry amendments. Eda et al. have reported that electrical properties of GQDs are size tunable. According to their findings of density functional theory (DTF), the band gap of GQDs consisting of 20 aromatic rings is approximately 2 eV, while for a benzene ring the value is 7 eV [54]. GQDs are a very new addition to the family of quantum dots and a great deal is left to explore their electronic and electrochemical properties. Graphene has been widely explored in field-effect transistors but GQDs are applied in single electron transistor (SET)-based charge sensors [55–57]. SETs are newer switching devices that use controlled electron tunneling to amplify a current [58]. Apart from charge variation detection, GQDs are applied for electronic sensors for humidity detection based on the modulation of electron tunneling distances caused by humidity and pressure.

3.2. Absorption and photoluminescence properties

GQDs are widely explored for their photoluminescence properties. They generally show a strong absorbance in UV region. The basic absorption spectra of GQDs show a prominent peak at about 230 nm, which is assigned to the $\pi \rightarrow \pi^*$ excitation of the π bonds of aromatic C=C, and a shoulder peak at 300 nm is assigned to the n–π^* transition of C=O bonds [59]. GQDs also exhibit size-dependent UV–Vis absorption spectrum due to quantum confinement effect. Peng et al. [60] analyzed that the absorbance peak red shifted from 270 nm to 330 nm, with increase in the size from 1–4 nm to 7–11 nm (Figure 8a). It was also observed that varying the average size of GQDs from 5 nm to 35 nm, the peak energy of the absorption spectra monotonously decreases from 6.2 ev to 4.6 ev (Figure 8b) [61]. According to the findings of Fuyuno et al., the absorption spectra of GQDs showed increases in absorbance with decreasing wavelength for each sample. GQD samples were collected via high-performance liquid chromatography (HPLC) at different intervals. A gradual change in the absorption spectra of HPLC-GQDs was observed depending on the retention time (i.e., with the size of the GQDs). For the GQD samples collected at 4 h, no distinct energy gap and peak structure were obtained, while for the GQDs of 7 h and 10 h, peak structures were observed at ~300 nm, which corresponds to n–π^* transitions of nonbonding electrons in the C=O bonds (Figure 8c). However, the size dependency was not visible and the absorbance peaks were independent of size variation from 1.7 nm to 21 nm with GQDs prepared via glucose carbonization [62]. Moreover, absorption spectra also vary with difference in the method of synthesis [63, 64]. The presence of oxygen-containing groups also plays a governing role in the absorption peak position of

http://dx.doi.org/10.5772/61932

GQDs, as illustrated in Figure 8d. The two electronic transitions at 300 nm (3.81 eV) in the absorption spectra of the GQDs can be attributed to electronic transitions from s and p orbitals or from highest occupied molecular orbital (HOMO) to lowest unoccupied molecular orbital (LUMO) [65].

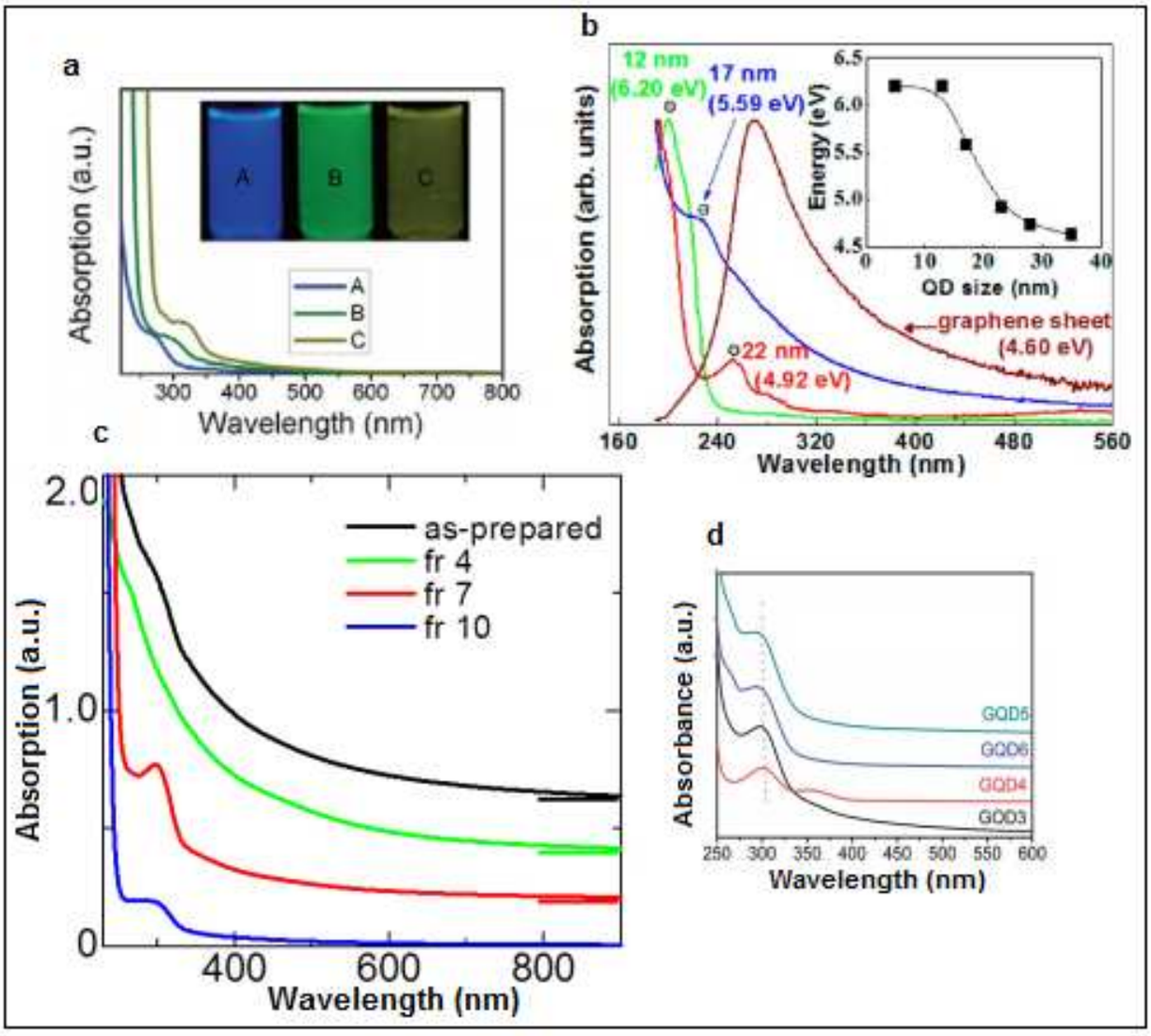

Figure 8. Variation in absorption spectra of GQDs with synthesis parameters (a) UV–Vis spectra of GQDs A, B, and C correspond to synthesized reaction temperature at 120, 100, and 80°C, respectively (Ref [60]: Peng et al.); (b) Absorption spectra for three typical GQDs of 12, 17, and 22 nm average sizes dispersed in DI water and a graphene sheet. Inset: absorption peak energy as a function of average GQD size (Ref [61]: Kim et al.); (c) Spectra of different sizes of GQDs at different collection times (4, 7, 10 h) (Ref [62]: Fuyuno et al.); (d) Presence of oxygen functional groups variation and its effect on UV spectra (Ref [65]: Yang et al.)

Another attractive feature of GQDs is their photoluminescence profile. Though the exact mechanism of PL is still not completely validated, researchers have revealed that the possible causes can be quantum confinement effect, aromatic structures, presence of functional groups and oxygen-containing groups, free zigzag sites, and edge defects, due to which GQDs show

new absorption features that affect the photoluminescence profile of GQDs [66–69]. It is a well-known fact that GQDs exhibit quantum confinement and edge effects, the key players of PL properties. Researchers have identified that the band gap is a function of size of QDs and decreases with an increase in size. Eda et al. [55] in their hypothesis proposed that the radiative recombination of e–h pairs generated within localized states can be the possible cause of blue PL spectra. The energy gap between the π and π^* states generally depends on the size of sp^2 clusters [27] or conjugation length [18]. According to their findings, it is the interaction between the nanometer-sized sp^2 clusters and the finite-sized molecular sp^2 domains which is the key in optimizing the blue emission. Moreover, the synthesis procedure of GQDs in top-down approaches and cutting of large graphene fragments in different crystallographic directions generates edges (zigzag and arm chair). These edges are prima facie responsible for diverse emission properties, as suggested by Kim et al. [61]. Zigzag sites are either carbine like with a triplet ground state or carbyne-like with a singlet ground state, and the irradiation decay of activated electrons from LUMO to HOMO is the most probable cause of blue emission [14].

In this segment, we will discuss some aspects of GQDs and their effect on PL spectra. Size dependency of PL of GQDs was reported by Alam et al. [70]. In their analysis, emission wavelengths of pristine zigzag-edged GQDs of different diameters were calculated. On varying the size from 0.46 nm to 2.31 nm, GQDs exhibited PL spectra from deep UV to near infrared as shown in Figure 9a. The smallest GQD (benzene) showed an emission peak at 235.2 nm while a peak at 999.5 nm was exhibited by GQDs of size 2.31 nm. They reported a linear and steep size dependence and concluded that emission covers the entire visible-light spectrum (400–770 nm) on varying the diameter of GQD from 0.89 nm to 1.80 nm [70].

Depending on the method of synthesis, GQDs possess oxygen-containing groups, that is, hydroxyl, carboxy, carbonyl, and epoxy ether groups; the difference in energy levels of surface groups and emission traps on GQDs governs the difference in emission spectra and PL with different colors including red, green, blue, and yellow [52, 71].

As reported by Zhu et al., surface defects on GQDs that arise from oxidation of surface groups also result in red-shifted PL spectra [72].In addition, not only the surface defects and functional groups but also the synthesis parameters (pH and solvent), size, and excitation wavelength have marked their impact on the PL spectra of GQDs. As described above, quantum confinement effect is a major phenomenon of QDs that arises when the size of QDs is less than the Bohr exciton radius. This size dependency of band gap of GQDs is responsible for their unique optical and spectroscopic characteristics. It is reported that by decreasing the size of QDs, emission spectra show blue or high energy shift [73–76]. Figure 9 illustrates various effects of physiological parameters on emission spectrum of GQDs.

In an interesting finding, few reports deal with the upconversion luminescence properties exhibited by GQDs. As reported by Shen et al., surface-passivated GQDs showed strong upconversion PL when illuminated with 980 nm. An unconverted PL spectrum at 525 nm was obtained (Figure 10a). The upconversion emissions also showed peak shifts from 390 nm to 460 nm when excited with wavelengths of 600–800 nm. They further demonstrated that the PL spectrum was a transition from the lowest unoccupied molecular orbital to the highest occupied molecular orbital [23]. Similar phenomena were also observed by Zhu et al., and

http://dx.doi.org/10.5772/61932

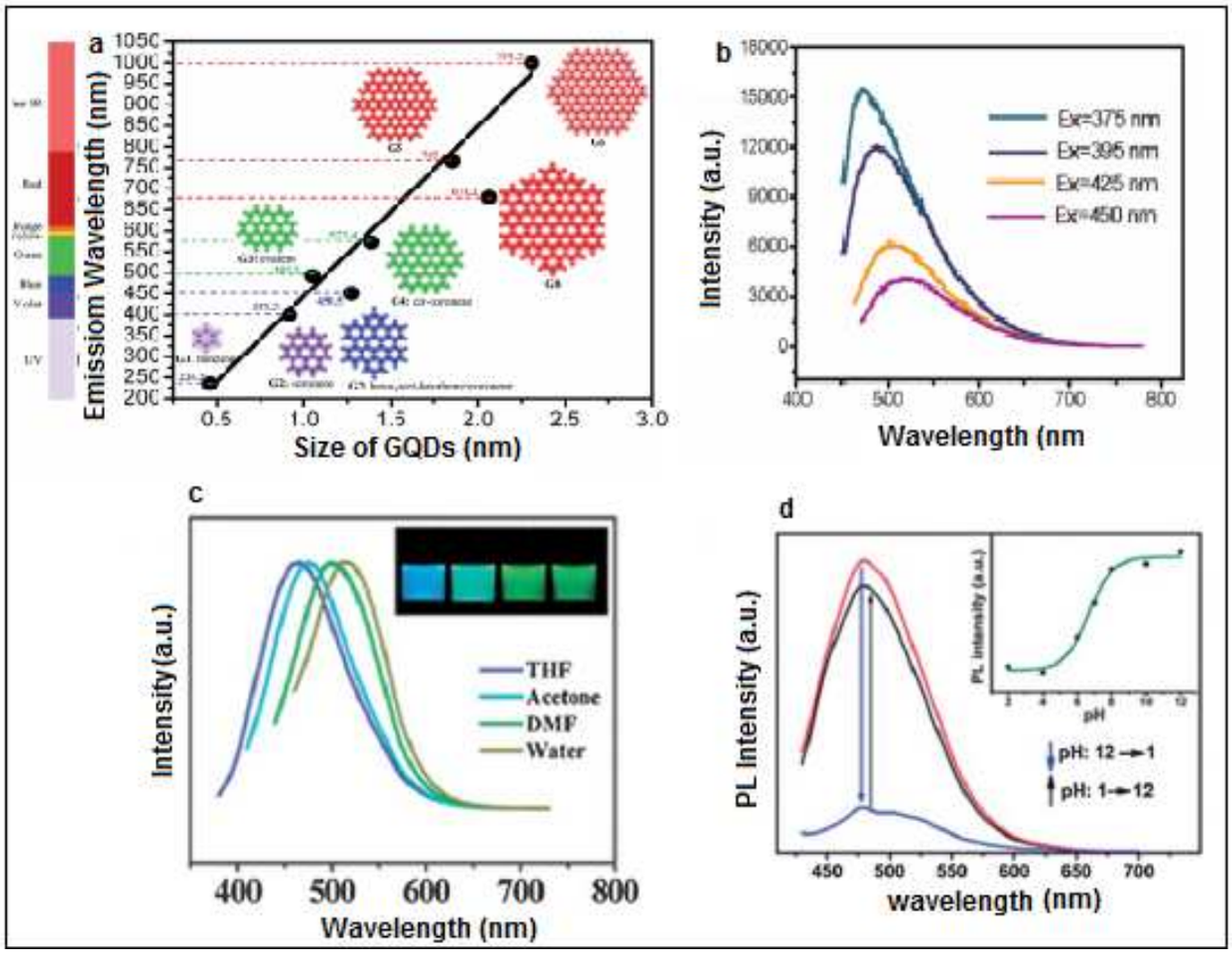

Figure 9. Illustrating the change in emission spectra of GQDs based on (a) size (Ref [70]: Alam et al.); (b) Excitation dependent (Ref [71]: Tang et al.); (c) in different solvents (Ref [75], Zhu et al.); (d) with pH of the GQD solution (Ref [15]: Pan et al.)

when their GQDs were illuminated with 600–900 nm wavelengths, a significant red shift was obtained. The possible cause for this can be explained by the multi-photon active process as reported for carbon dots earlier [77, 78]. The possible cause of upconversion effect was depicted by anti-Stokes transition, as shown in Figure 10c. In comparison to excitation-dependent upconversion effect, Zhou et al. observed an excitation-independent upconversion effect with GQDs synthesized via ultrasonication as illustrated in Figure 10d [79].

3.3. Quantum yield

Quantum yield is another important aspect associated with the PL of GQDs. The highest value reported was 28%. However, Wu et al. have reported a high QY of ~55% by the pyrolysis method of GQD synthesis [43]. In general, the QY depends on the fabrication methods and surface chemistry. It was reported by Liu et al. and Loh and coworkers that the removal of oxygen-containing groups and surface passivation can drastically enhance the QY of GQDs [80–82]. The possible reasons for this can be the non-radiative electron–hole recombination

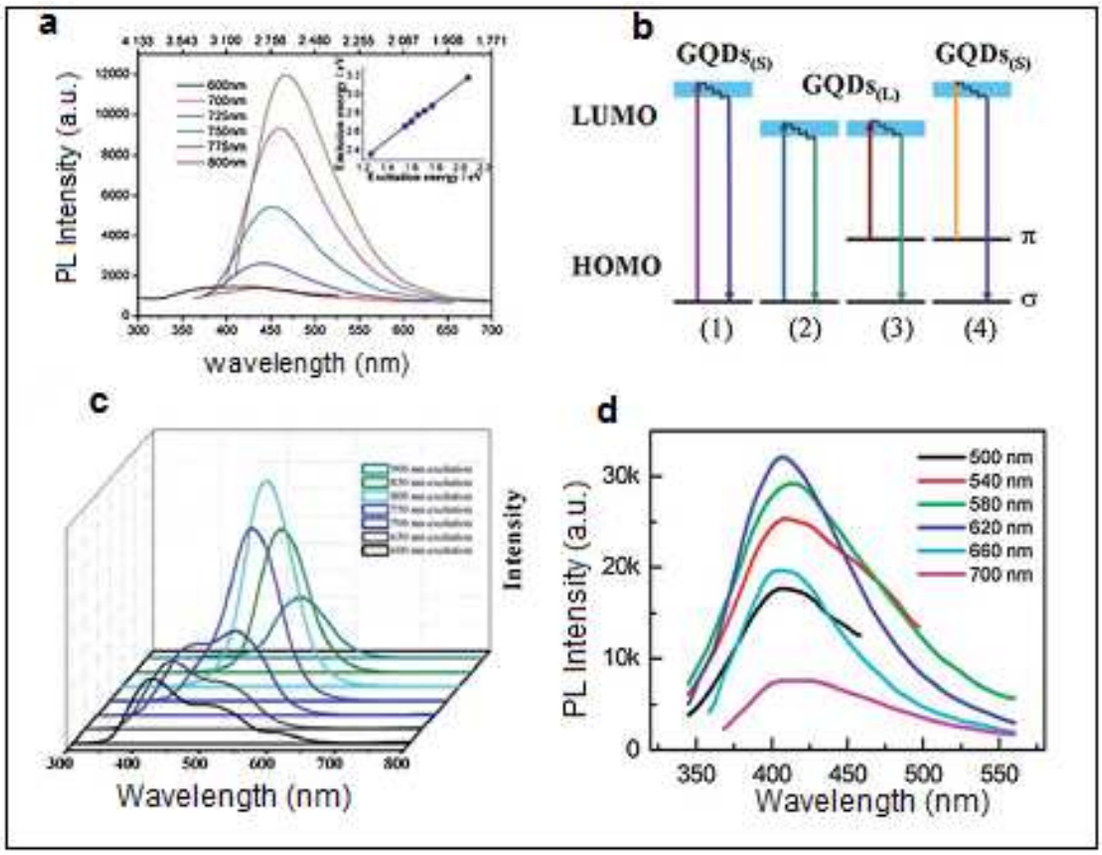

Figure 10. (a) Upconversion luminescence properties exhibited by GQDs; (b) A schematic illustration of various typical electronic transitions processes of GQDs (Ref [23]: Shen et al.) (c) PL spectra of GQDs upconversion GQDs on illumination of 600–900 nm (Ref [78]: Zhu et al.); (d) Upconverted excitation-independent PL spectra of the ultrasonically synthesized GQDs at different excitation (Ref [79]: Zhou et al.)

tendency of oxygen-containing groups. Though GQDs have optical properties similar to semiconductor QDs, few basic differences in PL spectra in terms of bandwidth (GQDs have broad bandwidth) and spectral shift toward red that decreases with increasing excitation clearly distinguish them from the semiconductor QDs [82].

3.4. Electrochemiluminescence

Another unique characteristic of GQDs is electrochemiluminescence (ECL), a phenomenon of showing luminescence during electrochemical reactions. GQDs are electro-active species and few reports deal with their ECL properties [83, 84]. Figure 11 is an illustration of ECL and PL spectra of GQDs synthesized by hydrothermal method. GQDs exhibited bright blue emission under ultraviolet irradiation (~365 nm) in a water solution of neutral pH, an excitation-independent photoluminescence feature, and interestingly, it also exhibited a novel anodic ECL by using H_2O_2 as a co-reactant [83]. The possible mechanism can be the formation of excited-state GQDs* through electron transfer (ET) annihilation of negatively and positively radical species.

http://dx.doi.org/10.5772/61932

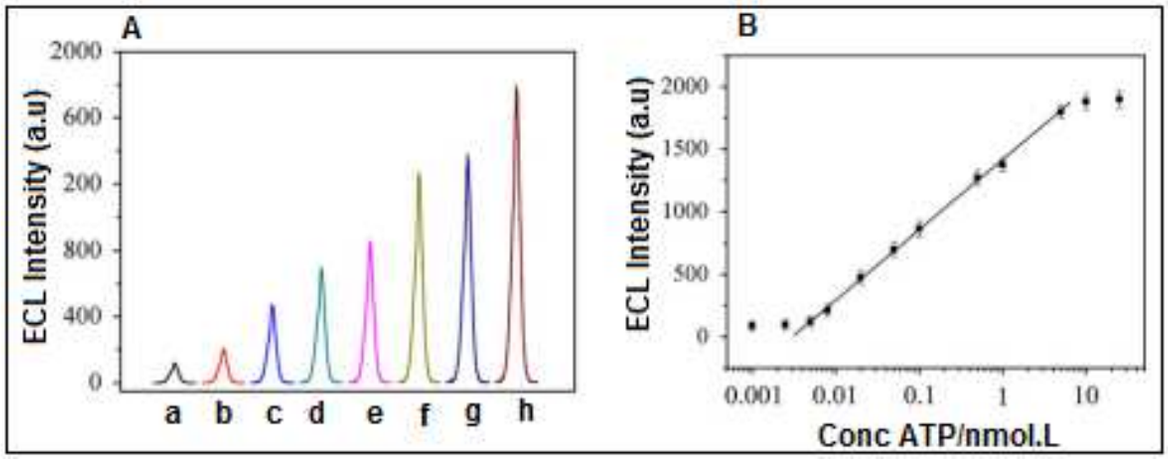

Figure 11. ECL intensity curves at different ECL intensities and ATP concentration. (Ref [83]: Lu et al.)

3.5. Biocompatibility of GQDs

GQDs are basically carbon materials and show low toxicity. As graphene and related materials have shown great potential in disease diagnosis and bioimaging, the potential toxicity of GQDs in biological systems has become a cause of concern. It is previously reported that graphene or graphene oxide can cause pulmonary inflammation upon inhalation [55], and graphene family materials were found to be toxic to bacteria [85–87]. In vitro studies on animal cell lines were also conducted and it was reported that the cytotoxicity of graphene and GQDs is also dependent on the method of synthesis and starting material. GQDs synthesized from carbon nanotubes are more toxic than those synthesized from graphene oxide and amino acids. Few reports have shown that GQDs can be well tolerated at low concentrations (50 μg/ml) but at higher concentrations (1 mg/ml), they show acute toxicity. In this regard, it is imperative to find out new strategies for less-toxic graphene materials for their practical biological applications with enhanced bioavailability. Surface functionalization of GQDs and graphene material can play an important role in mitigating the cytotoxicity of GQDs. These are the materials of future with potential biomedical applications, and surface modification of GQDs is an important criterion for their wide applicability. Many researchers have reported the emergence of unique properties with variations in surface properties. Production of reactive oxygen species (ROS) from GQDs by blue laser ablation and surface passivation by polyethylene glycol was reported by Christensen et al. in cell-free conditions [88] In another study by Yuan and coworkers, on functionalized GQDs, very encouraging results of cytotoxicity were observed; even at higher concentrations (200 μg/ml), quantum dots showed good biocompatibility as depicted in Figure 12 a, b. Their analysis proved that surface functionalization can be a better alternative to reduce the cytotoxity of GQDs [89]. Jastrzębska et al. have summarized the toxicological analysis of graphene-related materials in a recent review [90]. As an interesting fact, many researchers have reported that GQDs are less toxic than GO and the possible cause may be less damage to cell membrane owing to their smaller size and their fast clearance [91].

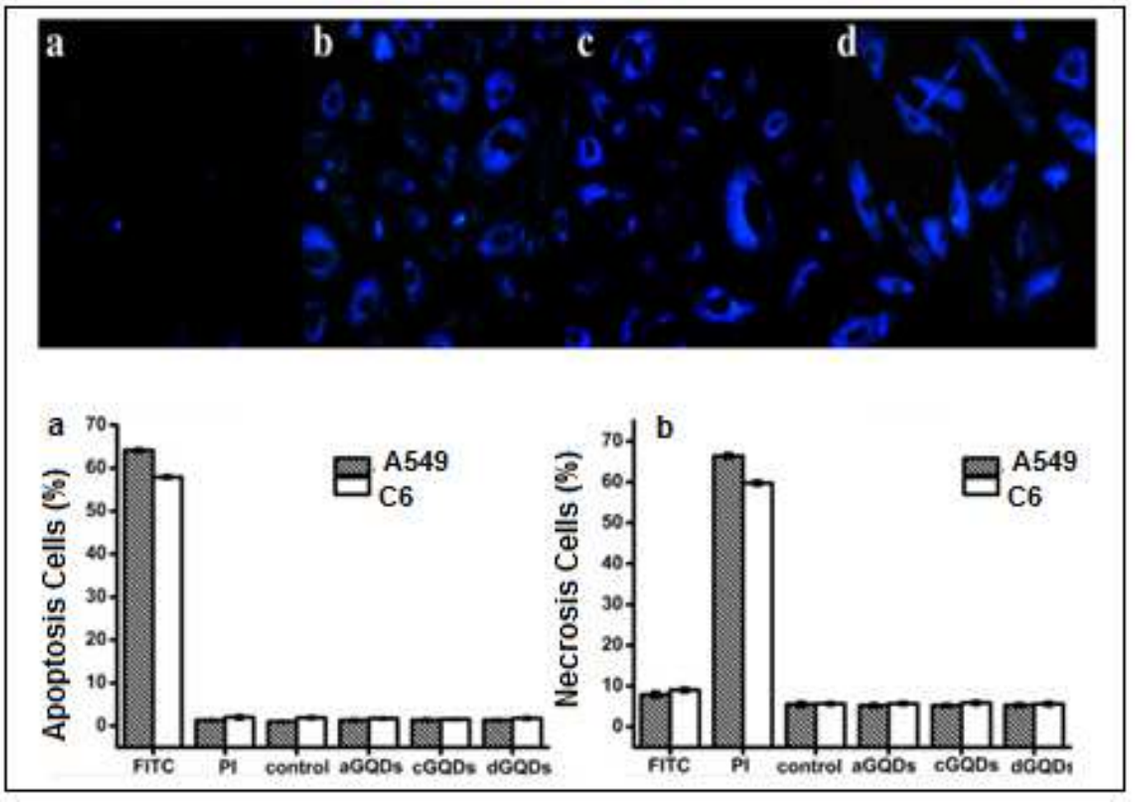

Figure 12. Biocompatibility analysis of GQDs in vitro. (Ref [89]: Yuan et al.)

Moreover, due to increasing biological applications of GQDs and graphene materials, in vivo toxic effects should also be considered. Wang et al. have reported that high doses (0.4 mg) of graphene oxide caused chronic toxicity in animals [91, 92]. In another study, PEGylated GQDs showed no toxicity to mice while PEG–GO was toxic due to its accumulation in liver and spleen. They observed dark spots of micrometer size, much larger than the size of GO in animal organs. That was a clear indication of aggregation of PEG–GO in organs, responsible for organ damage and even deaths [93].

Based on the data available, it can be concluded that GQDs are less toxic than other graphene family materials and that is the prime reason for newer applications of GQDs in the field of biology and medicine.

4. Nanotheranostic applications of GQDs

Due to the excellent optical and physical properties of GQDs, they have wide biological applications as a sensitive probe for disease marker screening in fluids, precise marker for tissue biopsy classification, and high-resolution contrast agent for biomedical cell/tissue imaging that can be applied for detecting tiny tumors. Moreover, the most distinctive feature of GQDs is their precise detection from macroscale visualization, down to atomic resolution using electron microscopy. Though many reports are there dealing with the wide applications

of GQDs in energy-related [94, 95] biosensing [96, 97] and light-emitting diodes [98, 99], in this section we will only emphasize the role of GQDs in drug delivery and bioimaging or specifically nanotheranostic application of GQDs in medical biology. "Theranostics" is a new term coined by Funkhouser in 2002 that describes any "material that combines the modalities of therapy and diagnostic imaging" into a single package [100].

With the advancement in the field of nanotechnology, the field of nanotheranostics has emerged that not only provides a platform for simultaneous drug distribution and release monitoring but also enables us to evaluate the therapeutic efficacy of a noninvasive treatment in real time that will guide toward personalized therapy based on patients' individual responses and needs, minimizing the chances of the adverse side effects due to over- or underdosing [101, 102].

In this segment, recent advances in the application of graphene quantum dots in drug delivery and bioimaging will be discussed.

4.1. Drug delivery applications

GQDs are emerging as an effective drug carrier for nanotheranostics application due to their unique properties as quantum dots as well as goodness of graphene. To date, many reports deal with GQDs as drug carrier and bioimaging. Recently, Wang et al. [103] synthesized PEGylated green fluorescent GQDs for carrying doxorubicin (Dox) for cancer treatment. Surface passivation by PEG enhanced the fluorescence and improved the solubility of GQDs. Moreover, GQDs were synthesized via reduction of GO by L-ascorbic acid so they adopted the green route for better biocompatibility. Figure 13a represents the schematic of Dox-loaded GQDs. GQD–PEG showed distinctly different loading capacities toward Dox at different pH values. The maximum loading capacity of Dox on GQD–PEG is 0.9 mg/mg at pH 5.5; 2.5 mg/mg at pH 7.4; and 1.1 mg/mg at pH 9 (Figure 13b, c).

In another similar application, Zhu et al. [104] fabricated paclitaxel-loaded multifunctional core–shell structure capsules composed of olive oil, dual-layer porous TiO2 shell, Fe_3O_4, and GQDs. The olive oil core for hydrobhic drug loading was the novel aspect of this formulation. The TiO_2 shell suppressed the initial burst release, while Fe_3O_4 and GQDs were utilized for magnetic targeting and fluorescence imaging, respectively. In two different interesting applications, DNA cleavage activity with drug delivery of GQDs was reported. Wang et al. [105] prepared GQD–Dox complex for enhanced nucleus accumulation and DNA cleavage efficiency. They achieved efficient delivery of doxorubicin to the nucleus through Dox/GQD conjugates, as the conjugates assumed different cellular and nuclear internalization pathways compared to free Dox. Furthermore, with drug-resistant cancer cells, the Dox/GQD conjugates increased the nuclear uptake and cytotoxicity of Dox, capable of increasing the chemotherapy efficacy of anticancer drugs that are suboptimal due to the drug resistance. Figure 14 shows the DNA cleavage activity and cellular internalization of GQD–Dox complex via diffusion and the release of drug in nucleus after interaction with DNA. In another approach, Zhou et al. [106] have reported GQDs in DNA cleavage system. According to their findings, by using GQDs and Cu^{2+}, about 90% supercoiled DNA was converted into nicked DNA, while only about 59% supercoiled DNA was cleaved with the same amount of large-sized GO and Cu^{2+}.

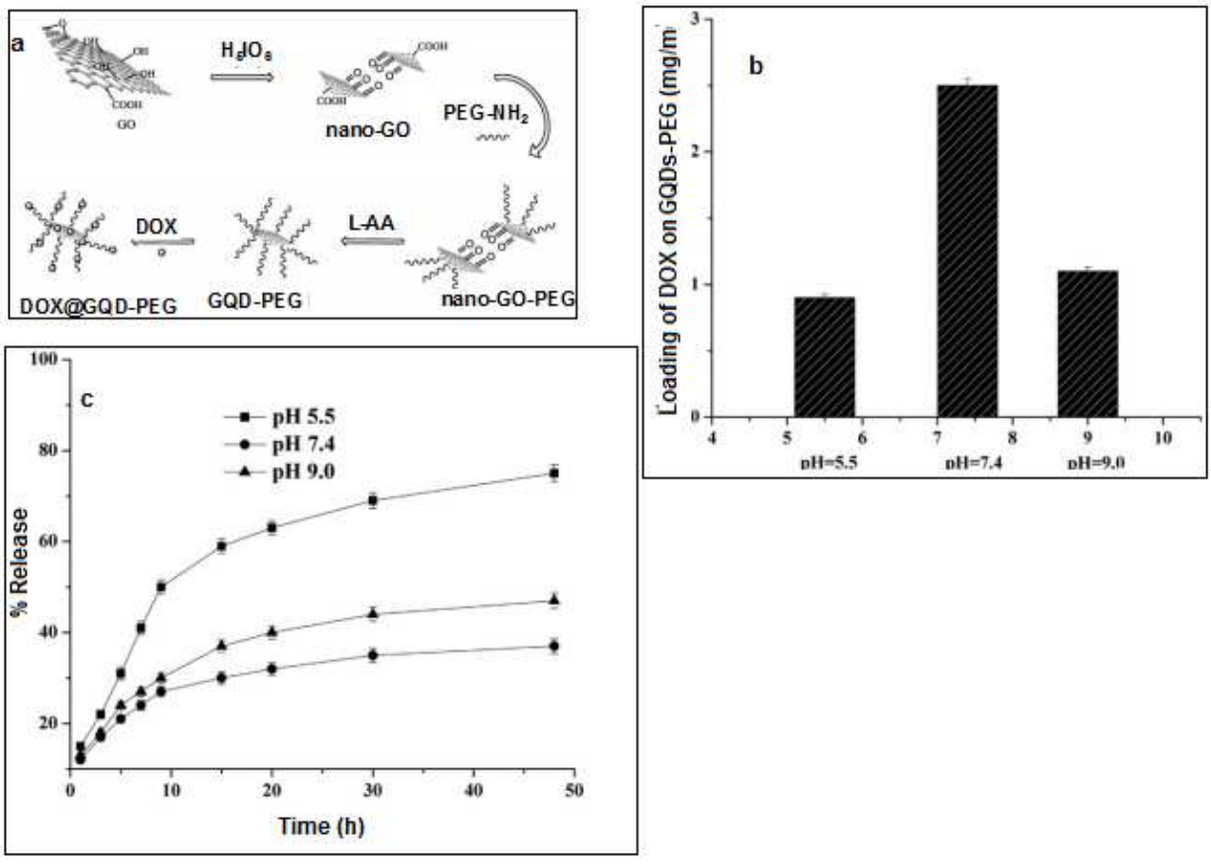

Figure 13. (a) Illustration of drug loading on GQDS; (b) Drug loading capacity of GQDs; (c) Percentage release profile of drugs at different pH. (Ref [103]: Wang et al.).

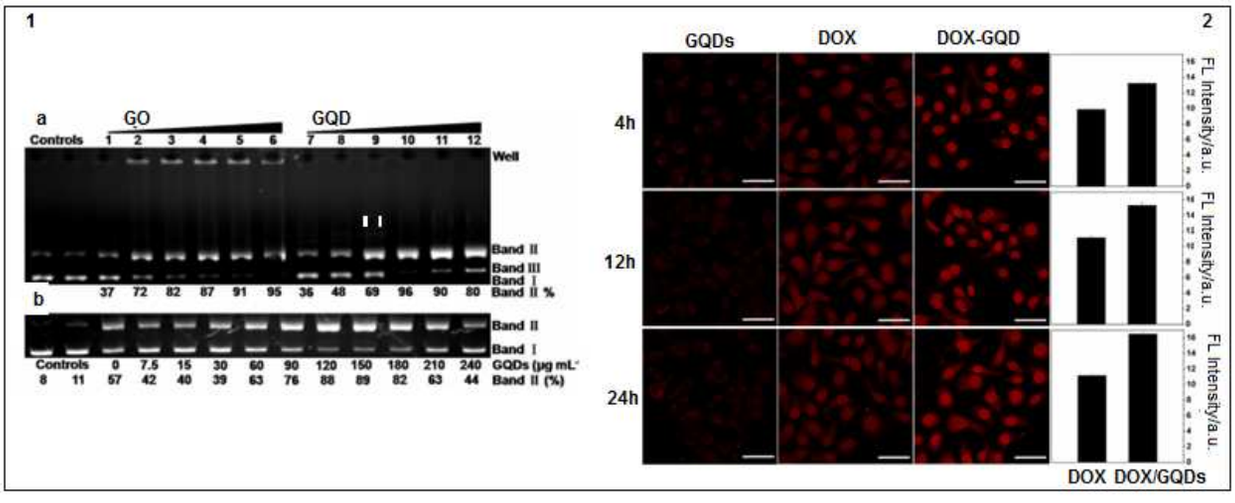

Figure 14. (a) Illustrating DNA (38 μM) cleavage with Cu $(Phen)_2$ (di-1,10-phenanthroline-copper) with GO and GQDs; 1(b) Cleavage with different concentrations of GQDS and DOX. 2: CLSM images of MCF-7 cells incubated with GQDs, DOX and GQD-DOX. (Ref [105]: Wang et al.)

According to their hypothesis, the as-prepared GQD sheets with smaller lateral size performed as a better intercalator to DNA molecules than micron GO sheets and therefore, under the same conditions, GQDs exhibited better efficiency than GO for DNA cleavage.

A nanocomposite based on conglomeration of Au–Fe_3O_4 core–shell with GQDs is reported by Oza et al. [107]. This modular design enabled Au-Fe_3O_4-GQD-based magnetic combined therapeutic nanoplatform to perform multiple functions simultaneously, such as in multimodal imaging, drug delivery, and real-time monitoring. Dox was loaded by cystamine linker and the drug release was a temperature-dependent phenomenon. With folic acid (FA) as the targeted moiety, this formulation showed potential to be developed as an efficient drug delivery system. Another FA-mediated Dox-loaded GQD-based targeted delivery system was reported by Wang et al. [108]. Due to the inherent fluorescence of GQDs, cell movement in real time can be easily monitored without employing external dyes, and simultaneous localization of the drug carrier and the loaded drug can be possible. The nanoassembly was internalized by the target cells via receptor-mediated endocytosis with prolonged Dox release and accumulation. Though there are many reports utilizing folic acid as targeting moieties for cancer-cell-specific drug delivery, the major constraint is that folic acid receptor is overexpressed on healthy cells as well that restricts the applicability of FA-functionalized delivery system. Nahain et al. [109] put forth a new targeting strategy by functionalizing GQDs with hyaluronic acid (HA). HA is a natural polysaccharide and a targeting receptor for CD44 cells. CD44 are cancer stem cells responsible for drug resistance and reoccurrence of pancreatic cancer. Hence, by targeting CD44 by HA, an effective targeting strategy was developed. Figure 15 illustrates Dox-loaded green fluorescent GQD nanoformulation. The authors also evaluated the in vivo efficacy of GQDs in bioimaging and therapy. Figure 15b shows the in vivo imaging of mice model studies performed. HA-functionalized GQDs showed enhanced stability and stable fluorescence in vivo that could pave the way for future applications of GQDs in targeted drug delivery for cancer, the most fatal disease of human history (Figure 16b).

4.2. Bioimaging applications

Traditional semiconductor quantum dots like CdSe or CdS and their core–shell nanoparticles have been exploited for applications in in vitro and in vivo cell imaging [110, 111], but the toxicity and potential health and environmental hazards associated with them restrict their applicability in live systems. In this regard, GQDs with their tunable PL, ecofriendly nature, and emergence of GQDs to date have shown remarkable potential for their successful application in the field of biotechnology and medicine owing to their excellent optical properties and low cytotoxicity up to very high concentrations of 400 μg/ml [112]. The authors also noted good uptake of GQDs by cells, as shown by the bright PL observed. Another example of bioimaging potential of GQDs, made from CX-72 carbon black, was reported by Dong et al. [113] in human breast cancer MCF-7 cells. They obtained effective luminescence inside the cell nucleus along with the cell membrane and cytoplasm. It was the first example that illustrated that GQDs have the ability to penetrate the cell nucleus and is another promising feature of GQDs to prove their strong candidature in nanotheranostic applications (Figure 16a). Sun et al. [114] compared the cytotoxicity and bioimaging capabilities of chemically reduced and

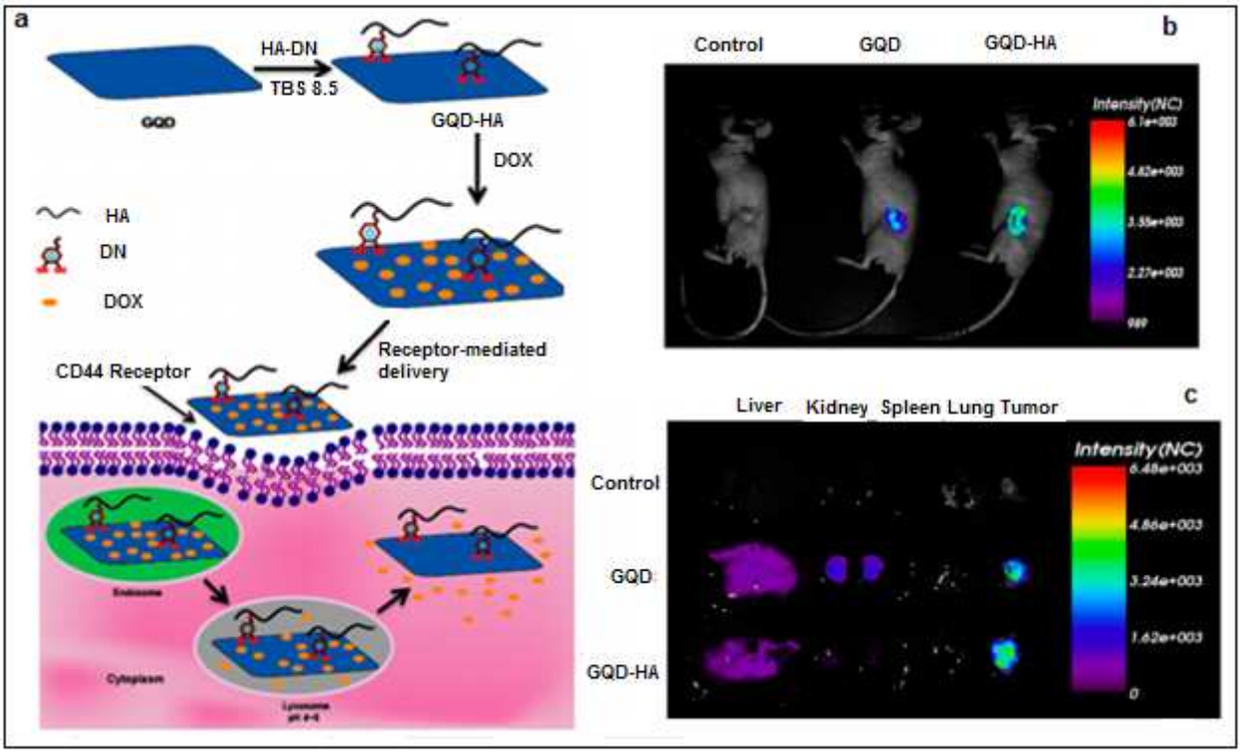

Figure 15. (a) Schematic of target delivery of GQDs using hyaluronic acid and subsequent release of the drug from the surfaces of GQD in a tumor-cell environment; (b) In vivo fluorescence images of GQD-HA in mice after tail vein injection; (c) Ex vivo images of liver, kidney, spleen, heart, and tumor after dissection. (Ref [109]: Nahin et al.)

photoreduced brightly blue luminescent GQDs in A549 cells using the MTT (3-(4,5-dimethylthiazol-2-yl)-2,5-diphenyltetrazolium bromide) assay. According to their findings, the cytotoxicity of the chemically reduced GQDs (cGQDs) was significantly greater than that of the photoreduced GQDs (pGQDs). The possible reason for this was the use of toxic reagents ($NaBH_4$ and $N_2H_4 \times H_2O$) during the chemical reduction. Photoreduced GQDs also exhibited stronger fluorescence indicating better cellular uptake due to the presence of less negative charge on the GQD surface. A very interesting approach was presented by Zhang et al. [35] by utilizing GQDs to label stem cells. The ability of GQDs to penetrate stem cell without reducing cell viability was exploited. Three different types of stem cells (neurosphere cells (NSCs), pancreas progenitor cells (PPCs), and cardiac progenitor cells (CPCs)) with GQDs at a final concentration of 25 μg/ml were labeled and strong fluorescence was observed in the cytoplasm of the stem cells, but not in the nuclei. They obtained good penetration into cytoplasmic areas but not inside the cell nucleus. The authors also found that the GQDs were able to easily penetrate tumor cells (human lung cancer (A549) and human breast cells (MCF-7) and showed little cytotoxicity (Figure 16b). In most of the cases, downconversion PL imaging is reported, but Zhu et al. came up with upconversion GQDs. In downconversion, mainly UV or blue excitations are involved that are considered unsafe for living systems. In this scenario, Zhu et al. could attain more biocompatibility with their upconversion GQDs excited at near-infrared light of wavelength 808 nm for illuminating mouse osteoblast precursor cell line

http://dx.doi.org/10.5772/61932

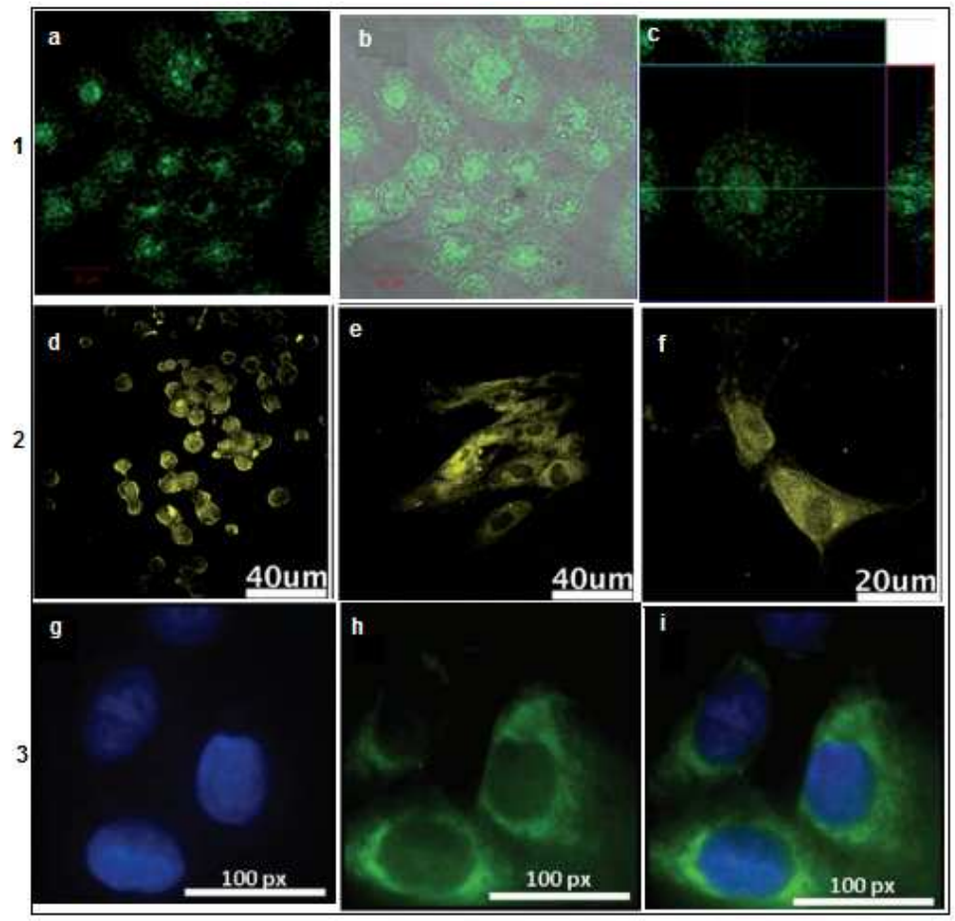

Figure 16. Confocal Images of MCF-7 cells labeled with GQDs 1 (a) Fluorescent image; (b) Bright field; (c) Merged fluorescent and bright field; (d) Section analysis (Ref [114]: Dong et al.); 2. Stem cells images of (d) Neurospheres cells (NSCs); (e) Pancreas progenitor cells (PPCs); (c) Cardiac progenitor cells (CPCs) (Ref [35] Zhang et al.); 3. High-contrast bioimaging via GQDs for breast cancer cell line (T47D). (Ref [9]: Peng et al.)

(MT3T3) cells. A blue or bright green fluorescence was observed inside the cells even after 20 min of continuous excitation. This indicated the successful internalization of GQDs inside the cells and photostability of GQDs as well [115].

Recently, Nigam et al. [20] have also reported the excellent bioimaging potential in a human serum-albumin-based multifunctional drug delivery system for pancreatic cancer. A strong and stable green fluorescence with good biocompatibility was observed in their analysis. In another report, Peng et al. [9] incubated breast cancer cell line T47D. The cell nucleus was stained with DAPI (blue color). Figure 16c illustrates the images of T47D cells treated with green GQDs with a 4-h incubation time, which clearly visualized the phase contrast image of T47D cells with nucleus stained with blue DAPI and green fluorescence from the cytoplasm. This bioimaging data proved that GQDs can be utilized in high-contrast bioimaging applications. Recently, GQDs synthesized by polycyclic aromatic compound via bottom-up approach by Zhou et al. were applied for illuminating MCF-7 (breast cancer cell lines). A stable green fluorescence inside the cytoplasm was obtained [116].

Zheng et al. have demonstrated a novel application of GQDs for insulin receptor dynamics, using total internal reflection fluorescence microscopy (TIRFM), by functionalizing insulin with GQDs [117]. According to their observation, small discrete clusters of GQDs after pre-incubating adipocytes with insulin GQDs were detected. The steady lateral movement of GQD-enlightened clusters to the cell membrane and vertical movement between the inner cytosol and the plasmalemmal region were also tracked by following the GQD fluorescence (Figure 17). This application is a good example of the potential of the edge-functionalized GQDs for investigating dynamic cellular processes.

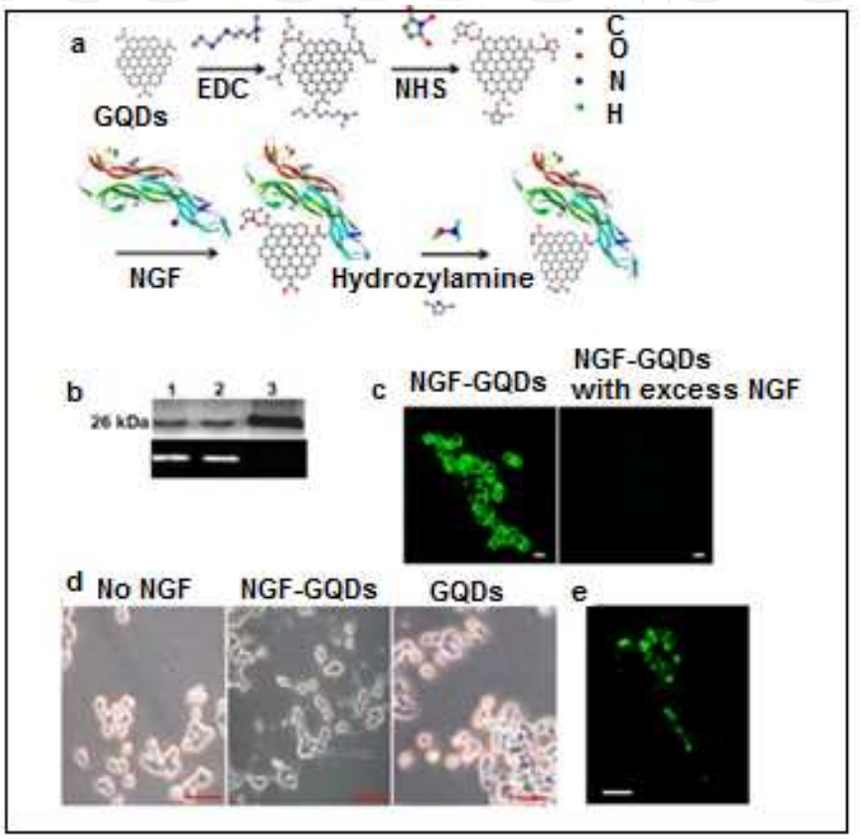

Figure 17. (a) Schematic illustration of conjugating a GQD with NGF; (b) Gel electrophoresis of NGF-GQD (lane 1), FITC-NGF (lane 2), and NGF (lane 3); (c) Fluorescence images of living PC12 cells incubated with 200 ng/mL NGF–GQDs (left) or NGF–GQDs together with 20 μg/mL free NGF (right) for 15 min; (d) Representative phase-contrast images of PC12 cells after 2-day incubation; (e) Distribution of NGF–GQDs in PC12 cells differentiated by 200 ng/mL NGF–GQDs for 24 h. (Ref [117]: Zheng et al.)

GQDs are gradually attaining popularity for their in vivo applications also. The basic flaw related with in vivo imaging is background signal associated with autofluorescence of animal tissues. Moreover, the Rayleigh scattering of short wavelength light absorbed by water is another undesirable effect that is to be considered. It was reported by Nurunnabi et al. that carboxylated GQDs can be efficiently explored for superficial tissue imaging but short-wavelength excitation limits their use for deep tissue bioimaging [118]. However, With GQDs of near-infrared photoluminescence, after 8 h of GQD injection, fluorescent signals were

http://dx.doi.org/10.5772/61932

obtained near heart, spleen, and kidney [119]. In another approach, Ge and coworkers synthesized GQDs with polythiophene derivatives via hydrothermal approach and they observed an emission wavelength of 680 nm that enables these GQDs for in vivo applications. Another important finding of their work was the application of as-synthesized GQD in photodynamic therapy as it was observed that GQDs could produce $^1O_2$ via multistate sensitization process (Figure 18) with a quantum yield of about 1.3, the highest yield reported for photodynamic therapy (PDT) agents to date [120].

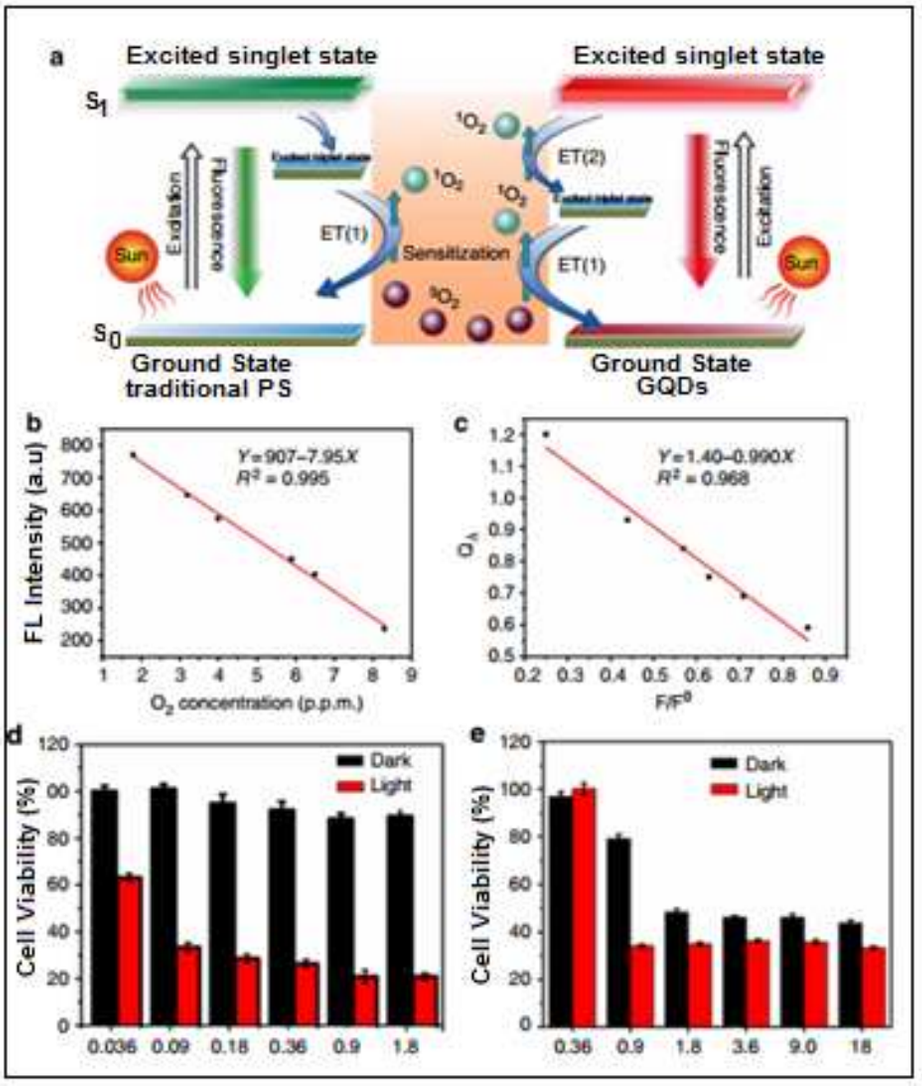

Figure 18. (a) Schematic illustration of the $^1O_2$ generation mechanisms by conventional PDT agents (left) and GQDs (right); (b) Fluorescence intensity of GQDs at 680 nm versus the O_2 concentration in solution; (c) The dependence of the $^1O_2$ quantum yield (Q_Δ) on the fluorescence intensity ratio at 680 nm (F/F^0); (d) GQDs in the concentration range 0.036–1.8 μM; (e) Protoporphyrin (PpIX) in the concentration range 0.36–18 μM. (Ref [120]: Ge et al.)

Although the cytotoxicity of GQDs in cells has been reported to be relatively low, contradictory findings were reported by Markovic et al. [121]. According to their observation, GQDs could be cytotoxic to U251 human glioma cells. They postulate that the GQDs can induce oxidative

stress and activate apoptosis and autophagy-type cell deaths by generating reactive oxygen species (ROS).

5. Conclusion and future prospects

GQDs have attracted tremendous interest in various fields like biotechnology, electronics, and medicine due to their excellent optical and physical properties, biocompatibility, and chemical stability. However, the research on GQDs is still in nascent state and there is huge scope to further explore the applicability of GQDs. The major issues related with GQDs are low quantum yield, low productivity, surface chemistry, and size tunability, and lack of control over PL and optical properties. However, irrespective of these drawbacks, GQDs represent an optimistic future for carbon materials. In our speculation, the future research on GQDs will be based on the following aspects.

Advancement in synthesis approaches

Low production yield is the major problem associated with GQDs. Hence, the development of better synthesis strategies by solvent selection, reaction conditions, and appropriate cutting methodology in top-down approaches and better size and solubility control in bottom-up methods should be explored.

Multifunctionality of GQDs

To extend the applicability of GQDs in bioimaging and drug delivery, novel approaches are to be developed. Still there are very few reports dealing with in vivo imaging and drug delivery mediated with multifunctional GQDs. Based on their application potential, it is imperative to explore the newer techniques for generating functionalized GQDs for their application in MRI and CT scan.

Quantum yield enhancement

To date, the GQDs with QY ranging from 10% to 55% have been reported. To increase the QY and PL efficiency of GQDs, new surface-passivation strategies are needed so that GQDs with better bioimaging and stable fluorescence can be obtained.

Applicability in newer areas

There is no report to date on application of GQDs in brain. A great deal can be done by tuning the excitation and emission properties of GQDs and they can be potentially exploited for blood–brain barrier penetration and brain gene therapy for neurodegenerative diseases.

Toxicological evaluation

Toxicity of nanoparticles is an area of growing research. GQDs are a new addition in the family of nanoparticles and there are concerns about the possible side effects associated with GQDs. So biodistribution, organ accumulation, and genotoxicity of GQDs synthesized via different methods, shapes, sizes, and surface groups should be evaluated.

Graphene quantum dots have shown a high potential in such a short span of time. The ongoing research in this field will open new vistas that will revolutionize the future of medical and biotechnology applications.

Acknowledgements

Author Dr Preeti Nigam Joshi is thankful to the Department of Science and Technology, Government of India, for providing financial support as INSPIRE Faculty Award grant.

Author details

Preeti Nigam Joshi[1*], Subir Kundu[2], Sunil K. Sanghi[3] and Dhiman Sarkar[1]

*Address all correspondence to: ph.joshi@ncl.res.in; nigampreeti@gmail.com

1 Combichem Bioresource Center, National Chemical Laboratory, Pune, India

2 School of Biochemical Engineering, Indian Institute of Technology, Varanasi, India

3 Microfluidics and MEMS Center, Advance Materials and Process Research Institute, Bhopal, India

References

[1] Novoselov KS, Geim AK, Morozov SV, Jiang D, Zhang Y, Dubonos SV, Grigorieva V, Firsov A. Electric field effect in atomically thin carbon films. Science. 2004; 306: 666–669. DOI:10.1126/science.1102896.

[2] Novoselov KS, Geim AK, Morozov SV, Jiang D, Katsnelson MI, Grigorieva IV, Dubonos SV, Firsov AA. Two-dimensional gas of massless Dirac fermions in graphene. Nature. 2005; 438: 197–200. DOI:10.1038/nature04233.

[3] Wallace PR. The band theory of graphite. Phu. Rev. 1947; 71: 622. DOI:http://dx.DOI.org/10.1103/PhysRev.71.622.

[4] Boehm HP, Clauss A, Fischer GO, Hofmann U, Anorg Z. Das Adsorptionsverhalten sehr dünner Kohlenstoff-Folien. Allg. Chem. 1962; 316: 119–127. DOI:10.1002/zaac.19623160303.

[5] Mouras S, Hamwi A, Djurado D, Cousseins JC. Synthesis of first stage graphite intercalation compounds from fluoride. Rev. Chim. Miner. 1987; 24: 572–582.

[6] Li LS, Yan X. Collioidal quantum dots. J. Phys. Chem. Lett. 2010; 1: 2572–2576. DOI: 10.1021/jz100862f.

[7] Ye R, Peng Z, Metzger A, Lin J, Mann JA, Huang K, Xiang C, Fan X, Samuel ELG, Alemany LB, Marti AA, Tour JM. Bandgap engineering of coal-derived graphene quantum dots. ACS Appl. Mater. Interface. 2015; 7: 7041–7048. DOI:10.1021/acsami. 5b01419.

[8] Mueller, X Yan, JA McGuire, L Li. Triplet states and electronic relaxation in photoexcited graphene quantum dots. Nano Lett. 2010; 10: 2679–2682. DOI:10.1021/ nl101474d.

[9] Peng J, Gao W, Gupta BK, Liu K, Romero-Aburto R, Ge L, Song L, Alemany LB, Zhan X, Gao G, Vithayathil SA, Kaipparettu B, Marti AA, Hayashi T, Zhu TT, Ajayan PM. Graphene quantum dots derived from carbon fibers. Nano Lett. 2012; 12: 844–849. DOI:10.1021/nl2038979.

[10] Yan X, Cui X, Li B, Li L. Large, solution-processable graphene quantum dots as light absorbers for photovoltaics. Nano Lett. 2010; 10: 1869–1873. DOI:10.1021/nl101060h.

[11] Dutta M, Sarkar S, Ghosh T, Basak D. ZnO/Graphene quantum dot solid-state solar C \cell. J. Phys. Chem. C. 2012; 116: 20127–20131. DOI:10.1021/jp302992k.

[12] Gupta V, Chaudhary N, Srivastava R, Sharma GD, Bhardwaj R, Chand S. Luminescent graphene quantum dots for organic photovoltaic devices. J. Am. Chem. Soc. 2011; 133: 9960–9963. DOI:10.1021/ja2036749.

[13] Dong Y, Shao J, Chen C, Li H, Wang R, Chi Y, Lin X, Chen G. Blue luminescent graphene quantum dots and graphene oxide prepared by tuning the carbonization degree of citric acid. Carbon. 2012; 50: 4738–4743. DOI:10.1016/j.carbon.2012.06.002.

[14] Pan DY, Zhang JC, Li Z, Wu MH. Hydrothermal route for cutting graphene sheets into blue-Luminescent graphene quantum dots. Adv Mater. 2010; 22: 734–738. DOI: 10.1002/adma.200902825.

[15] Pan D, Guo L, Zhang L, Xi C, Xue Q, Huang H, Li J, Zhang Z, Yu W, Chen Z, Zu M. Cutting sp^2 clusters in graphene sheets into colloidal graphene quantum dots with strong green fluorescence. J. Mater. Chem. 2012; 22: 3314–3318. DOI:10.1039/ C2JM16005F.

[16] Yan X, Li B, Cui X, Wei Q, Tajima K, LS Li. Independent tuning of the band gap and redox potential of graphene quantum dots. J. Phys. Chem. Lett. 2011 ; 2: 1119–1124. DOI:10.1021/jz200450r.

[17] Tetsuka H, Asahi R, Nagoya A, Okamoto K, Tajima I, Ohta R, Okamoto A. Optically tunable amino-functionalized graphene quantum dots. Adv. Mater. 2012; 24: 5333–5338. DOI:10.1002/adma.201201930.

[18] Feng Q, Cao QQ, Li M, Liu FC, Tang NJ, Du YW. Synthesis and photoluminescence of fluorinated graphene quantum dots. Appl. Phys. Lett. 2013; 102: 013111–013114. DOI:10.1063/1.4774264.

[19] Hu CF, Liu YL, Yang YH, Cui JH, Huang ZR, Wang YL, Yang LF, Wang HB, Xiao Y, Rong JH. One-step preparation of nitrogen-doped graphene quantum dots from oxidized debris of graphene oxide. J. Mater. Chem. B. 2013; 1: 39–42. DOI:10.1039/C2TB00189F.

[20] Zhang ZH, Wu PY. Hydrothermal aggregation induced crystallization: a facial route towards polycrystalline graphite quantum dots with blue photoluminescence. Cryst. Eng. Comm. 2012; 14: 7149–7152. DOI:10.1039/C2CE26117K.

[21] Liu Y, Wu PY. Graphene quantum dot hybrids as efficient metal-free electrocatalyst for the oxygen reduction reaction. ACS Appl. Mater. Interface. 2013; 5: 3362–3369. DOI:10.1021/am400415t.

[22] Nigam P, Waghmode S, Louis M, Wangnoo S, Chavan P, Sarkar D. Graphene quantum dots conjugated albumin nanoparticles for targeted drug delivery and imaging of pancreatic cancer. J. Mater. Chem. B. 2014; 2: 3190–3195. DOI:10.1039/C4TB00015C.

[23] Shen J, Zhu Y, Chen C, Yang X, Li C. Facile preparation and upconversion luminescence of graphene quantum dots. Chem. Commun. 2011; 47: 2580–2582. DOI:10.1039/C0CC04812G.

[24] Zhu SJ, Zhang JH, Qiao CY, Tang SJ, Li YF, Yuan WJ, Li B, Tian L, Liu F, Hu R, Gao HN, Wei HT, Zhang H, Sun HC, Yang B. Strongly green-photoluminescent graphene quantum dots for bioimaging applications. Chem. Commun. 2011; 47: 6858–6860. DOI:10.1039/C1CC11122A.

[25] Zhu SJ, Zhang JH, Liu X, Li B, Wang XF, Tang SJ, Meng QN, Li YF, Shi C, Hu R, Yang B. Graphene quantum dots with controllable surface oxidation, tunable fluorescence and up- conversion emission. RSC Adv. 2012; 2: 2717–2720. DOI:10.1039/C2RA20182H.

[26] Shin Y, Park J, Hyun D, Yang J, Lee J, Kim J, Lee H. Acid-free and oxone oxidant-assisted solvothermal synthesis of graphene quantum dots using various natural carbon materials as resources. Nanoscale. 2015; 7: 6533–5637. DOI:10.1039/C5NR00814J.

[27] Chan CF, Lau SP, Luk CM, Tsang MK. Two-photon fluorescence in N-doped graphene quantum dots. Int. J. Chem. Nucl. Mater. Metall. Eng. 2014: 8; 1313–1316.

[28] Luo Z, Yang D, Qi G, Shang J, Yang H, Wang Y, Yuwen L, Yu T, Huang W, Wang L. Microwave-assisted solvothermal preparation of nitrogen and sulfur co-doped reduced graphene oxide and graphene quantum dots hybrids for highly efficient oxygen reduction. J. Mat. Chem. A. 2014; 2: 20605–20611. DOI:10.1039/C4TA05096G.

[29] Tang L, Ji R, X C, Lin L, Jiang H, Li X, Teng KS, Luk CM, Zeng S, Hao J, Lau SP. Deep ultraviolet photoluminescence of water-soluble self-passivated graphene quantum dots. ACS Nano. 2012; 6: 5102–3110. DOI:10.1021/nn300760g

[30] Li LL, Ji J, Fei R, Wang CZ, Lu Q, Zhang JR, Jiang LP, Zhu JJ. A facile microwave avenue to electrochemiluminescent two-color graphene quantum dots. Adv. Funct. Mater. 2012; 22: 2971–2979. DOI:10.1002/adfm.201200166.

[31] Zhu Y, Wang G, Jiang H, Chen L, Zhang X. One-step ultrasonic synthesis of graphene quantum dots with high quantum yield and their application in sensing alkaline phosphatase. Chem. Commun. (Camb). 2015; 5: 948–951. DOI:10.1039/c4cc07449a.

[32] Lu J, Yang JX, Wang J, Lim A, Wang S, Loh KP. One-pot synthesis of fluorescent carbon nanoribbons, nanoparticles, and graphene by the exfoliation of graphite in ionic liquids. ACS Nano. 2009; 3: 2367–2375. DOI:10.1021/nn900546b.

[33] Zheng L, Chi Y, Dong Y, Lin J, Wang B. Electrochemiluminescence of water-soluble carbon nanocrystals released electrochemically from graphite. J. Am. Chem. Soc. 2009; 131: 4564–4565. DOI:10.1021/ja809073f.

[34] Li Y, Hu Y, Zhao Y, Shi G, Deng L, Hou Y, Qu L. An Electrochemical avenue to green-luminescent graphene quantum dots as potential electron-acceptors for photovoltaics. Adv. Mater. 2011; 23: 776–780. DOI:10.1002/adma.201003819.

[35] Zhang M, Bai L, Shang W, Xie W, Ma H, Fu Y, Fang D, Sun H, Fan L, Han M, Liu C, Yang S. Facile synthesis of water-soluble, highly fluorescent graphene quantum dots as a robust biological label for stem cells. J. Mater. Chem. 2012; 22: 7461–7467. DOI: 10.1039/C2JM16835A.

[36] Shinde DB, Pillai VK. Electrochemical preparation of luminescent graphene quantum dots from multiwalled carbon nanotubes. Chem. Eur. J. 2012; 18: 12522–12528. DOI: 10.1002/chem.201201043.

[37] Shinde DB, Dhavle VM, Kurungot S, Pillai VM. Electrochemical preparation of nitrogen-doped graphene quantum dots and their size-dependent electrocatalytic activity for oxygen reduction. Bull. Mater. Sci. 2015; 38: 435–442. DOI:10.1007/s12034-014-0834-3.

[38] Tan X, Li Y, Li X, Zhou S, Fan L, Yang S. Electrochemical synthesis of small-sized red fluorescent graphene quantum dots as a bioimaging platform. Chem. Comm. 2015; 51: 2544–2546. DOI:10.1039/C4CC09332A.

[39] Ponomarenko LA, Schedin F, Katsnelson MI, Yang R, Hill EW, Novoselov KS, Geim AK. Chaotic dirac billiard in graphene quantum dots. Science. 2008; 320: 356–358. DOI:10.1126/science.1154663.

[40] Lee J, Kim K, Park WI, Kim BH, Park JH, Kim TH, Bong S, Kim CH, Chae G, Jun M, Hwang Y, Jung YS, Jeon S. Uniform graphene quantum dots patterned from self-assembled silica nanodots. Nano Lett. 2012; 12: 6078–6083. DOI:10.1021/nl302520m.

[41] Liu R, Wu D, Feng X, Müllen K. Bottom-up fabrication of photoluminescent graphene quantum dots with uniform morphology. J. Am. Chem. Soc. 2011; 133: 15221–15223. DOI:org/10.1021/ja204953k.

[42] Liu JJ, Zhang XL, Cong ZX, Chen ZT, Yang HH, Chen GN. Glutathione-functionalized graphene quantum dots as selective fluorescent probes for phosphate-containing metabolites. Nanoscale. 2013; 5: 1810–1815. DOI:10.1039/C3NR33794D.

[43] Wu X, Tian F, Wang W, Chen J, Wub M, Zha JX. Fabrication of highly fluorescent graphene quantum dots using L-glutamic acid for in vitro/in vivo imaging and sensing. J. Mat. Chem. C. 2013; 1: 4676–4684. DOI:10.1039/C3TC30820K.

[44] Wang L, Wang Y, Xu T, Yao C, Liu Y, Li Z, Chen Z, Pan D, Sun L, Wu M. Gram-scale synthesis of single-crystalline graphene quantum dots with superior optical properties. Nat. Commun. 2014; 5: 1–9. DOI:10.1038/ncomms6357.

[45] Lin L, Rong M, Lu S, Song X, Zhong Y, Yan J, Wang Y, Chen Xi. A facile synthesis of highly luminescent nitrogen-doped graphene quantum dots for the detection of 2,4,6-trinitrophenol in aqueous solution. Nanoscale. 2015; 7: 1872–1878. DOI:10.1039/C4NR06365A.

[46] Lu J, Yeo PSE, Gan CK, Wu P, Loh KP. Transforming C_{60} molecules into graphene quantum dots. Nat. Nanotechnol. 2011; 6: 247–252. DOI:10.1038/nnano.2011.30.

[47] Sinclair J, Dr. Dagotto, "An introduction to quantum dots: confinement, synthesis, artificial atoms and applications," Solid State II Lecture Notes, University of Tennessee, Knoxville, 2009.

[48] Chukwuocha EO, Onyeaju MC, Harry TST. Theoretical studies on the effect of confinement on quantum dots using the Brus Equation. World J. Condens. Matter. Phys. 2012; 2: 96–100. DOI:10.4236/wjcmp.2012.22017.

[49] Dinadayalane TC, Leszczynski J. Remarkable diversity of carbon–carbon bonds: structures and properties of fullerenes, carbon nanotubes, and graphene. Struct. Chem. 2010; 21: 1155–1169. DOI:10.1007/s11224-010-9670-2.

[50] Geim A. Graphene: status and prospects. Science. 2009; 324: 1530–1534. DOI:10.1126/science.1158877.

[51] Allen MJ, Tung VC, Kaner RB. Honeycomb carbon: a review of graphene. Chem. Rev. 2010; 110: 132–145. DOI:10.1021/cr900070d.

[52] Li L, Wu G, Yang G, Peng J, Zhao J, Zhu JJ. Focusing on luminescent graphene quantum dots: current status and future perspectives. Nanoscale. 2013; 5: 4015–4039. DOI: 10.1039/C3NR33849E.

[53] Baker SN, Baker GA. Luminescent carbon nanodots: emergent nanolights. Angew. Chem. Int. Ed. 2010; 49: 6726–6744. DOI:10.1002/anie.200906623.

[54] Eda G, Lin YY, Mattevi C, Yamaguchi H, Chen HA, Chen IS, Chen CW, Chhowalla M. Blue photoluminescence from chemically derived graphene oxide. Adv. Mater. 2010; 22: 505–509. DOI:10.1002/adma.200901996.

[55] Güttinger J, Seif J, Stampfer C, Capelli A, Ensslin K, Ihn T. Time-resolved charge detection in graphene quantum dots. Phys. Rev. B. 2011; 83: 165445–165452. DOI:http://dx.doi.org/10.1103/PhysRevB.83.165445.

[56] Li HO, Tu T, Cao G, Wang LJ, Guo GC, Guo GP. Quantum transport in graphene quantum dots. Nanotechnology and nanomaterials: new progress on graphene research DOI:10.5772/52873.

[57] González JW, Delgado F, Fernández-Rossier J. Graphene single-electron transistor as a spin sensor for magnetic adsorbates. Phys. Rev. B. 2012; 87: 085433. DOI:http://dx.DOI.org/10.1103/PhysRevB.87.085433.

[58] Ihn T, Güttinger J, Molitor F, Schnez S, Schurtenberger E, Jacobsen A, Hellmüller S, Fery T, Ensslin K. Graphene single-electron transistors. Mater. Today. 2010; 13: 44–50. DOI:10.1016/S1369-7021(10)70033-X.

[59] Luo Z, Lu Y, Somers LA, Johnson ATC. High yield preparation of macroscopic graphene oxide membranes. J. Am. Chem. Soc. 2009; 131: 898–899. DOI:10.1021/ja807934n.

[60] Peng J, Gao W, Gupta BK, Liu Z, Ge RRL, Song L, Alemany LB, Zhan X, Gao G, Vithayathil SA, Kaipparettu BA, Marti AA, Hayashi T, Zhu JJ, Ajayan PM. Graphene quantum dots derived from carbon fibers. Nano Lett. 2012; 12: 844–849. DOI:10.1021/nl2038979.

[61] Kim S, Hwang SW, Kim MK, Shin DY, Shin DH, Kim CO, Yang SB, Park JH, Hwang E, Choi SH, Ko G, Sim S, Sone S, Choi HJ, Bae S, Hong BH. Anomalous behaviors of visible luminescence from graphene quantum dots: interplay between size and shape. ACS Nano. 2012; 6: 8203–8208. DOI:10.1021/nn302878r.

[62] Fuyuno N, Kozawa D, Miyauchi Y, Mouri S, Kitaura R, Shinohara H, Yasuda T, Komatsu N, Matsuda K. Size-dependent luminescence properties of chromatographically-separated graphene quantum dots. https://scirate.com/arxiv/1311.1684.

[63] Liu R, Wu D, Feng X, Muellen K. Bottom-Up Fabrication of photoluminescent graphene quantum dots with uniform morphology. J. Am. Chem. Soc. 2011; 133: 15221–15223. DOI:10.1021/ja204953k.

[64] Qu D, Zheng M, Zhang L, Zhao H, Xie Z, Jing X, Haddad RE, Fan H, Sun Z. Formation mechanism and optimization of highly luminescent N-doped graphene quantum dots. Sci. Rep. 2014; 4: 1–9. DOI:10.1038/srep05294.

[65] Yang F, Zhao M, Zheng B, Xiao D, Wu L, Guo Y. Influence of pH on the fluorescence properties of graphene quantum dots using ozonation pre-oxide hydrothermal synthesis. J. Mater. Chem. 2012; 22: 25471–25479. DOI:10.1039/C2JM35471C.

[66] Li H, He X, Liu Y, Huang H, Lian S, Lee ST, Kang Z. One-step ultrasonic synthesis of water-soluble carbon nanoparticles with excellent photoluminescent properties. Carbon. 2011; 49: 605–609. DOI:10.1016/j.carbon.2010.10.004.

[67] Li H, He X, Kang Z, Huang H, Liu Y, Liu J, Lian S, Tsang CHA, Yang X, Lee ST. Water-soluble fluorescent carbon quantum dots and photocatalyst design. Angew. Chem. Int. Ed. 2010; 49: 4430–4434. DOI:10.1002/anie.200906154.

[68] Qiao ZA, Wang Y, Gao Y, Li H, Dai T, Liu Y, Huo Q. Commercially activated carbon as the source for producing multicolor photoluminescent carbon dots by chemical oxidation. Chem. Commun. 2010; 46: 8812–8814. DOI:10.1039/C0CC02724C.

[69] Li H, Kang Z, Liu Y, Lee ST. Carbon nanodots: synthesis, properties and applications. J. Mater. Chem. 2012; 22: 24230–24253. DOI:10.1039/C2JM34690G.

[70] Mahasin Alam SK, Ananthanarayanan A, Huang L, Lim KH, Chen P. Revealing the tunable photoluminescence properties of graphene quantum dots. J. Mater. Chem. C. 2014; 2: 6954–6960. DOI:10.1039/C4TC01191K.

[71] Tang L, Ji R, Cao X, Lin J, Jiang H, Li X, Teng KS, Luk CM, Zeng S, Hao J, Lau SP. Deep ultraviolet photoluminescence of water-soluble self-passivated graphene quantum dots. ACS Nano. 2012 ; 6: 5102–5110. DOI:10.1021/nn300760g.

[72] Zhu S, Zhang J, Liu X, Li B, Wang X, Tang S, Meng Q, Li Y, Shi C, Hu R, Yang B. Graphene quantum dots with controllable surface oxidation, tunable fluorescence and up-conversion emission. RSC Adv. 2012; 2: 2717–2720. DOI:10.1039/C2RA20182H.

[73] Michalet X, Pinaud FF, Bentolila LA, Tsay JM, Doose S, Li JJ, Sundaresan G, Wu AM, Gambhir SS, Weiss S. Quantum dots for live cells, in vivo imaging, and diagnostics. Science. 2005; 307: 538–544. DOI:10.1126/science.1104274.

[74] Smith AM, Nie S. Semiconductor nanocrystals: structure, properties, and band gap engineering. Acc. Chem. Res. 2010; 43: 190–200. DOI:10.1021/ar9001069.

[75] Fan T, Zeng W, Tang W, Yuan C, Tong S, Cai K, Liu Y, Huang W, Min Y, Epstein AJ. Controllable size-selective method to prepare graphene quantum dots from graphene oxide. Nanoscale Res. Lett. 2015; 10: 55. DOI:10.1186/s11671-015-0783-9.

[76] Tian L, Liu F, Hu R, Gao H, Wei H, Zhang H, Sun H, YangB. Strongly green-photoluminescent graphene quantum dots for bioimaging applications. Chem. Commun. 2011; 47: 6858–6860. DOI:10.1039/C1CC11122A.

[77] Zhu S, Zhang J, Tang S, Qiao C, Wang L, Wang H, Liu X, Li B, Li Y, Yu W, Wang A, Sun H, Yang B. Surface chemistry routes to modulate the photoluminescence of gra-

phene quantum dots: From fluorescence mechanism to up-conversion bioimaging applications. Adv. Funct. Mater. 2012; 22: 4732–4740. DOI:10.1002/adfm.201201499.

[78] Shen WJ, Zhu Y, Chen C, Yang X, Li C. Facile preparation and upconversion luminescence of graphene quantum dots. Chem. Comm. 2011; 47: 2580–2582. DOI: 10.1039/C0CC04812G.

[79] Zhuo S, Shao M, Lee S. Upconversion and downconversion fluorescent graphene quantum dots: ultrasonic preparation and photocatalysis. ACS Nano. 2012; 6: 1059–1064. DOI:10.1021/nn2040395.

[80] Liu R, Wu D, Feng X, Muellen K. Bottom-up fabrication of photoluminescent graphene quantum dots with uniform morphology. J. Am. Chem. Soc. 2011; 133: 15221–15223. DOI:10.1021/ja204953k.

[81] Loh KP, Bao Q, Eda G, Chhowalla M. Graphene oxide as a chemically tunable platform for optical applications. Nat. Chem. 2010; 2: 1015–1024. DOI:10.1038/nchem.907.

[82] Pan D, Zhang J, Li Z, Wu M. Hydrothermal route for cutting graphene sheets into blue-luminescent graphene quantum dots. Adv. Mater. 2010; 22: 734–738. DOI: 10.1002/adma.200902825.

[83] Lu J, Yan M, Ge L, Ge S, Wang S, Yan J, Yu J. Electrochemiluminescence of blue-luminescent graphene quantum dots and its application in ultrasensitive aptasensor for adenosine triphosphate detection. Biosens. Bioelect. 2013; 47: 271–277. DOI:10.1016/j.bios.2013.03.039.

[84] Li LL, Ji J, Fei R, Wang CZ, Lu Q, Zhang JR, Jiang LP, Zhu JJ. A Facile microwave avenue to electrochemiluminescent two-color graphene quantum dots. Adv. Funct. Mater. 2012; 22: 2971–2979. DOI:10.1002/adfm.201200166.

[85] Hu W, Peng C, Luo W, Lv M, Li X, Li D, Huang Q, Fan C. Graphene-based antibacterial paper. ACS Nano. 2010; 4: 4317-4323. DOI:10.1021/nn101097v.

[86] Ruiz OR, Fernando KAS, Wang B, Brown NA, Luo PG, McNamara ND, Vangsness M, Sun Y, Bunker CE. Graphene oxide: a nonspecific enhancer of cellular growth. ACS Nano. 2011; 5: 8100–8107. DOI:10.1021/nn202699t.

[87] Zhang D, Liu X, Wang X. Green synthesis of graphene oxide sheets decorated by silver nanoprisms and their anti-bacterial properties. J. Inorg. Biochem. 2011; 105: 1181–1186. DOI:10.1016/j.jinorgbio.

[88] Christensen IL, Sun YP, Juzenas P. Carbon dots as antioxidants and prooxidants. J. Biomed. Nanotechnol. 2011; 7: 667–676. DOI:10.1007/s11434-013-6058.

[89] Yuan X, Liu Z, Guo Z, Ji Y, Jin M, Wang X. Cellular distribution and cytotoxicity of graphene quantum dots with different functional groups. Nanoscale Res. Lett. 2014; 9: 108. DOI:10.1186/1556-276X-9-108.

[90] Jastrzębska AM, Kurtycz P, Olszyna AR. Recent advances in graphene family materials toxicity investigations. J. Nanopart. Res. 2012; 14: 1320–1327. DOI:10.1007/s11051-012-1320-8.

[91] Wang A, Pu K, Dong B, Liu Y, Zhang L, Zhang Z, Duan W, Zhu Y. Role of surface charge and oxidative stress in cytotoxicity and genotoxicity of graphene oxide towards human lung fibroblast cells. J. Appl. Toxicol. 2013; 33: 1156–1164. DOI:10.1002/jat.2877.

[92] Wang K, Ruan J, Song H, Zhang J, Wo Y, Guo S, Cui D. Biocompatibility of graphene oxide. Nanoscale Res. Lett. 2011; 6: 1–8. DOI:10.1007/s11671-010-9751-6.

[93] Chong Y, Ma Y, Shen H, Tu X, Zhou X, Xu J, Dai J, Fan F, Zhang Z. The in vitro and in vivo toxicity of graphene quantum dots. Biomaterials. 2014; 35: 5041–5048. DOI: 10.1016/j.biomaterials.2014.03.021.

[94] Pan D, Xi C, Li Z, Wang L, Chen Z, Lu B, Wu M. Electrophoretic fabrication of highly robust, efficient, and benign heterojunction photoelectrocatalysts based on graphene-quantum-dot sensitized TiO_2 nanotube arrays. J. Mater. Chem. A. 2013; 1: 3551–3555. DOI:10.1039/C3TA00059A.

[95] Hamilton IP, Li B, Yan X, Li L. Alignment of colloidal graphene quantum dots on polar surfaces. Nano Lett. 2011; 11: 1524–1529. DOI:10.1021/nl200298c.

[96] Li X, Zhu S, Xu B, Ma K, Zhang J, Yang B, Tian W. Self-assembled graphene quantum dots induced by cytochrome c: a novel biosensor for trypsin with remarkable fluorescence enhancement. Nanoscale. 2013; 5: 7776–7779.

[97] Shi J, Chan C, Pang Y, Ye W, Tian F, Lyu J, Zhang Y, Yang Mo. A fluorescence resonance energy transfer (FRET) biosensor based on graphene quantum dots (GQDs) and gold nanoparticles (AuNPs) for the detection of mecA gene sequence of Staphylococcus aureus. Biosens Bioelectron. 2015; 67: 595–600. DOI:10.1016/j.bios.2014.09.059.

[98] Gupta V, Chaudhary N, Srivastava R, Sharma GD, Bhardwaj R, Chand S. Luminescent graphene quantum dots for organic photovoltaic devices. J. Am. Chem. Soc. 2011; 133: 9960–9963. DOI:10.1021/ja2036749.

[99] Luk CM, Tang LB, Zhang WF, Yu SF, Teng KS, Lau SP. An efficient and stable fluorescent graphene quantum dot–agar composite as a converting material in white light emitting diodes. J. Mater. Chem. 2012; 22: 22378–22381. DOI:10.1039/C2JM35305A.

[100] Funkhouser J. Reinventing pharma: the theranostic revolution. Curr. Drug Discov. 2002; 2: 17–25.

[101] Luk BT, Zhang L. Current advances in polymer-based nanotheranostics for cancer treatment and diagnosis. ACS Appl. Mater. Interface. 2014; 6: 21859–21873. DOI: 10.1021/am5036225.

[102] Lammers T, Kiessling F, Hennink WE, Storm G. Nanotheranostics and image-guided drug delivery: current concepts and future directions. Mol. Pharm. 2010; 7: 1899−1912. DOI:10.1021/mp100228v.

[103] Wang Z, Xia J, Zhou C, Via B, Xia Y, Zhanga F, Lia Y, Xia L, Tang J. Synthesis of strongly green-photoluminescent graphene quantum dots for drug carrier. Colloid Surf B Biointerface. 2013; 112: 192–196. DOI:10.1016/j.colsurfb.2013.07.025.

[104] Jing Y, Zhu Y, Yang X, Shen J, Li C. Ultrasound-triggered smart drug release from multifunctional core−shell capsules one-step fabricated by coaxial electrospray method. Langmuir. 2010; 27: 1175–1180. DOI:10.1021/la1042734.

[105] Wang C, Wu C, Zhou X, Han T, Xin X, Wu J, Zhang J, Guo S. Enhancing cell nucleus accumulation and DNA cleavage activity of anti-cancer drug via graphene quantum dots. Sci. Rep. 2013; 3: 2852. DOI:10.1038/srep02852.

[106] Zhou X, Zhang Y, Wang, Wu X, Yang Y, Zheng B, Wu H, Guo S, Zhang J. Photo-fenton reaction of graphene oxide: a new strategy to prepare graphene quantum dots for DNA cleavage. ACS Nano. 2012; 6: 6592–6599. DOI:10.1021/nn301629v.

[107] Oza G, Ravichandran OM, Velumani S, Ramirez JT, Garcia-Sierra F, Asomoza R. Designing a drug-delivery vehicle with Au-Fe3 O4 -graphene quantum dots: a tripronged mechanism for bioimaging, synaptic delivery and apoptosis induction in cancer cells. J. Nanomed. Nanotechnol. 2014; 5: 5. DOI.org/10.4172/2157-7439.S1.018.

[108] Wang X, Sun X, Lao J, He H, Cheng T, Wang M, WangS, Huang F. Multifunctional graphene quantum dots for simultaneous targeted cellular imaging and drug delivery. Colloid Surf. B Biointerface. 2014; 122: 638–644. DOI:10.1016/j.colsurfb.2014.07.043.

[109] Nahain AA, Lee JE, In I, Lee H, Lee KD, Jeong JH, Park SY. Target delivery and cell imaging using hyaluronic acid-functionalized graphene quantum dots. Mol. Pharm. 2013; 10: 3736−3744. DOI:10.1021/mp4003283.

[110] Vibin M, Vinayakan R, John A, Raji V, Rejiya CS, Vinesh NS, Abraham A. Cytotoxicity and fluorescence studies of silica-coated CdSe quantum dots for bioimaging applications. J. Nanopart. Res. 2011; 13: 2587–2596. DOI:10.1007/s11051-010-0151-8.

[111] Liu LW, Hu S, Pan Y, Zhang J, Feng Y, Zhang X. Optimizing the synthesis of CdS/ZnS core/shell semiconductor nanocrystals for bioimaging applications. Beilstein J. Nanotechnol. 2014; 5: 919–926. DOI:10.3762/bjnano.

[112] Zhu S, Zhang J, Qiao C, Tang S, Li Y, Yuan W, Li B, Tian L, Liu F, Hu R, Gao H, Wei H, Zhang H, Sun H, Yang B. Strongly green-photoluminescent graphene quantum dots for bioimaging applications. Chem. Commun. 2011; 47: 6858–6560. DOI:10.1039/C1CC11122A.

[113] Dong Y, Chen C, Zheng X, Gao L, Cui Z, Yang H, Guo C, ChI Y, Li CM. One-step and high yield simultaneous preparation of single- and multi-layer graphene quantum

dots from CX-72 carbon black. J. Mater. Chem. 2012; 22: 8764–8766. DOI:10.1039/C2JM30658A.

[114] Sun H, Wu L, Gao N, Ren J, Qu X. Improvement of photoluminescence of graphene quantum dots with a biocompatible photochemical reduction pathway and its bioimaging application. ACS Appl. Mater. Interface. 2013; 5: 1174–1179. DOI:10.1021/am3030849.

[115] Zhu S, Zhang J, Tang S, Qiao C, Wang L, Wang H, Liu X, Li B, Li Y, Yu W, Wang X, Sun H, Yang B. Surface chemistry routes to modulate the photoluminescence of graphene quantum dots: from fluorescence mechanism to up-conversion bioimaging applications. Adv. Funct. Mater. 2012; 22: 4732–4740. DOI:10.1002/adfm.201201499.

[116] Zhou L, Geng J, Liu B. Graphene quantum dots from polycyclic aromatic hydrocarbon for bioimaging and sensing of Fe^{3+} and hydrogen peroxide. Part. Part. Syst. Charact. 2013; 30: 1086–1092. DOI:10.1002/ppsc.201300170.

[117] Zheng XT, Than A, Ananthanaraya A, Kim DH, Chen P. Graphene quantum dots as universal fluorophores and their use in revealing regulated trafficking of insulin receptors in adipocytes. ACS Nano. 2013; 7: 6278–6286. DOI:10.1021/nn4023137.

[118] Nurunnabi M, Khatun Z, Huh KM, Park SY, Lee DY, Cho KJ, Lee Y. In vivo biodistribution and toxicology of carboxylated graphene quantum dots. ACS Nano. 2013; 7: 6858–6867. DOI 10.1021/nn402043c.

[119] Nurunnabi M, Khatun J, Reeck GR, Lee DY, Lee YK. Near infra-red photoluminescent graphene nanoparticles greatly expand their use in noninvasive biomedical imaging. Chem. Commun. 2013; 49: 5079–5081. DOI:10.1039/C3CC42334D.

[120] Ge J, Lan M, Zhou B, Liu W, Guo L, Wang H, Jia Q, Niu G, Huang X, Zhou, Meng X, Wang P, Lee CS, Zhang W, Han X. A graphene quantum dot photodynamic therapy agent with high singlet oxygen generation. Nat. Commun. 2014; 5 : 4596. DOI: 10.1038/ncomms5596.

[121] Markovic ZM, Ristic BZ, Arsikin KM, Klisic DG, Harhaji-Trajkovic LM, Todorovic-Markovic BM, Kepic DP, Kravic-Stevovic TK, Jovanovic SP, Milenkovic MM, Milivojevic DD, Bumbasirevic VZ, Dramicanin MD, Trajkovic VS. Graphene quantum dots as autophagy-inducing photodynamic agents. Biomaterials. 2012; 33: 7084–7092. DOI:10.1016/j.biomaterials.2012.06.060.

IntechOpen